Rb-Sr Age Estimates of Pore Fluids in Sedimentary Rocks, DGR Site, Kincardine, Ontario

Laurianne Bouchard

Thesis submitted to the
Faculty of Graduate and Postdoctoral Studies

In a partial fulfillment of the requirements for a

Masters of Sciences (M.Sc.)
in Earth Sciences

Ottawa-Carleton Geoscience Centre
and
University of Ottawa
Faculty of Science
Department of Earth Sciences

TABLE OF CONTENTS

LIST OF FIGURES

LIST OF TABLES

LIST OF ABREVIATIONS AND MINERALS

Acetic acid	AcOH
Albite	$NaAlSi_3O_8$
Ankerite	$Ca(Fe,Mg,Mn)(CO_3)_2$
Anorthite	$CaAl_2Si_2O_8$
Apatite	$Ca_5(PO_4)_3(OH,Cl,F)$
Biotite	$K(Mg,Fe)_3(OH,F)_2(Si_3AlO_{10})$
Calcite	$CaCO_3$
Celestite	$SrSO_4$
Chlorite	$(Fe,Mg,Al)_6(Si,Al)_4O_{10}(OH)_8$
Deep Geological Repository	DGR
Dolomite	$CaMg(CO_3)_2$
Gypsum	$CaSO_4{\cdot}2H_2O$
Hydrochloric acid	HCl
Hydrofluoric acid	HF
Illite	$(K,H_3O)(Al,Mg,Fe)_2(Si,Al)_4O_{10}[(OH)_2,(H_2O)]$
Meters Below Ground Surface	mBGS
Meters Linear Below Ground Surface	mLBGS
Muscovite	$KAl_2(AlSi_3O_{10})(F,OH)_2$
Nitric acid	HNO_3
Orthoclase	$KAlSi_3O_8$
Smectite	$(Na,Ca)_{0.3}(Al,Mg)_2Si_4O_{10}(OH)_2{\cdot}nH_2O$
Strontianite	$SrCO_3$
Vermiculite	$(Mg,Ca)_{0.7}(Mg,Fe,Al)_6(Al,Si)_8O_{22}(OH)_4{\cdot}8H_2O$
Water	H_2O

ABSTRACT

This study is part of a project aiming for the long-term burying of nuclear wastes in Kincardine, Ontario. Bedrock formations as well as their associated waters were analyzed in drill cores from the Michigan sedimentary basin, southwest Ontario.

This research utilizes geochemistry combined to strontium and rubidium isotope ratios in order to determine the origin of porewaters from Ordovician shales and limestones. It is demonstrated that these waters are the result of a mixing line between the Silurian (Guelph) and Cambrian groundwaters. This last end-member was also mixed with Precambrian brines to some extent.

Strontium and rubidium isotopes also demonstrated rubidium in clays were leached by porewaters over time. Once in solution, radioactive rubidium decayed into strontium over time. This process explains the accumulation of radiogenic strontium observed in porewaters.

An age estimate for the deposition of carbonates and other evaporates was calculated with the Rb-Sr isotope system. The calculated age is 453.7 million years before present for dolomites, which is consistent with the history of the site. It was possible to gen an approximate age of 339.7 million years for the formation of illites. This corresponds to the illitization process that occurred after the deposition of rocks, when the Silurian brines infiltrated the deeper Ordovician shale. It was also possible to estimate of porewaters ages.

Keywords: sedimentary rock; isotopes, strontium; rubidium; porewater.

RÉSUMÉ

L'étude des carottes de forage du bassin sédimentaire du Michigan, au sud-ouest de l'Ontario, a permis d'étudier les formations géologiques ainsi que les eaux qui y sont associées. Cette étude a été réalisée dans le cadre d'un projet ayant pour but l'enfouissement à long terme de déchets nucléaires à Kincardine, Ontario.

La recherche présentée dans cet ouvrage utilise la géochimie combinée aux ratios isotopiques de strontium et de rubidium, afin de déterminer l'origine des eaux interstitielles des schistes et calcaires ordoviciens. Il y est démontré que ces eaux sont le résultat d'un mélange entre les eaux souterraines du Silurien (Guelph) et Cambrien, cette dernière étant elle-même mélangée aux saumures datant du Précambrien.

L'analyse des ratios isotopiques de strontium et de rubidium ont également démontré que les eaux interstitielles ont lixivié une partie du rubidium des argiles. Une fois en solution, le rubidium radioactif s'est transformé en strontium radiogénique au fil du temps. Ce processus explique l'accumulation de ^{87}Sr dans les eaux interstitielles.

Le couple Rb-Sr a été utilisé pour la datation isotopique des carbonates et autres évaporites. L'âge calculé est de 453.7 millions d'années pour les dolomites, ce qui est consistant avec l'histoire géologique du site étudié. Il a également été possible d'obtenir un âge de formation pour les illites de 339.7 millions d'années. Ceci correspond au processus d'illitisation qui s'est déroulé bien après la déposition des roches, alors que les saumures du Silurien ont infiltré les schistes ordoviciens plus profonds. Enfin, le couple isotopique a permis d'obtenir une estimation de l'âge des eaux interstitielles.

Mots-clés: roche sédimentaire; isotopes; strontium; rubidium; eau interstitielle.

ACKNOWLEDGEMENTS

I could never thank enough Professor Ian Clark for giving me the chance to participate in this project, for his enthusiasm, patience, and support. You gave me the opportunity to surpass myself and to learn a science that changed the way I perceive our world. That is the greatest achievement I could have wished for. Thanks also for the two trips in Yukon; they were life-changing experiences. I was privileged to have you as supervisor. Thank you very much.

I would also like to thank my co-supervisor, Professor Jàn Veizer, for his help with the interpretation of data. Special thanks go to Pingqing Zhang and Nimal De Silva, whose precious help was required for ion analyzes, and to Sarah Murseli for her time and patience answering my thousands of questions about this project. I would also like to thank people from the Isotope Geochemistry and Geochronology Research Centre at Carleton University: Suangquan Zhang, Rhea Mitchell and Elizabeth Ann Spencer for their precious advice. This project could not have taken place without financial support from the University of Ottawa and the Nuclear Waste Management Organization. Many thanks!

Дзякуй to Natalia for all the good times, from Ottawa to Dawson City. I found in you a friend I wish to keep for a very long time. Le support de mes parents, de ma famille et de mes amis a été des plus précieux durant ces deux années. Je les remercie infiniment pour leurs encouragements. Merci de m'avoir encouragée à me dépasser, et de m'avoir soutenue dans les moments d'hésitation. Finalement, merci à François, mon Ché, pour tes conseils et ton support tout au long de cette aventure, pour m'avoir partagé ta folie et ta sagesse au quotidien. *Le plaisir est le bonheur des fous, le bonheur est le plaisir des sages.*

1.0 INTRODUCTION

This thesis study is part of a project initiated in 2002 by the Nuclear Waste Management Organization (NWMO), whose mandate is to propose approaches for the long-term management of used nuclear fuel. The report published by the organization in 2005 suggests burying the 200,000 cubic metres of low and intermediate level nuclear wastes in a deep-geological repository (DGR), 680 metres underneath the Bruce Power site in Kincardine, Ontario. Since then, feasibility and security assessments are being conducted, as the chosen site is just a few meters away from Lake Huron. The overall project involves many scientific disciplines such as geology, hydrogeology and chemistry, and also takes into consideration ethic and social dimensions to understand and address public perception. Various parameters have been studied since then to ensure minimal risk if nuclear wastes were to be buried.

1.1 Background

Safety assessment of the DGR includes studying the geology and hydrogeology of the site. Determining how rocks were formed helps understand their evolution, and studying water movements may provide details on the solute transport properties. Those are key elements to determine in such a project.

Amongst studied parameters were strontium concentrations and isotopes. Strontium is an abundant element in rocks and its isotopic ratio is widely used as an indicator of water-rock interaction and as a tracer for water movements (Clark & Fritz, 1997). In 2011, a few samples of rocks from the cores were leached with acetic acid to extract strontium. A few samples of porewaters and groundwaters were extracted along the cores and analyzed. Strontium isotopes ratios of rocks and waters at different depths

were plotted amongst the corresponding seawater line (Veizer, 1989). Although carbonates values of $^{87}Sr/^{86}Sr$ fell on the seawater line, porewaters showed enrichment starting from the early-Silurian to the Precambrian depths, as shown in Figure 1.1 (Raven, et al., 2011).

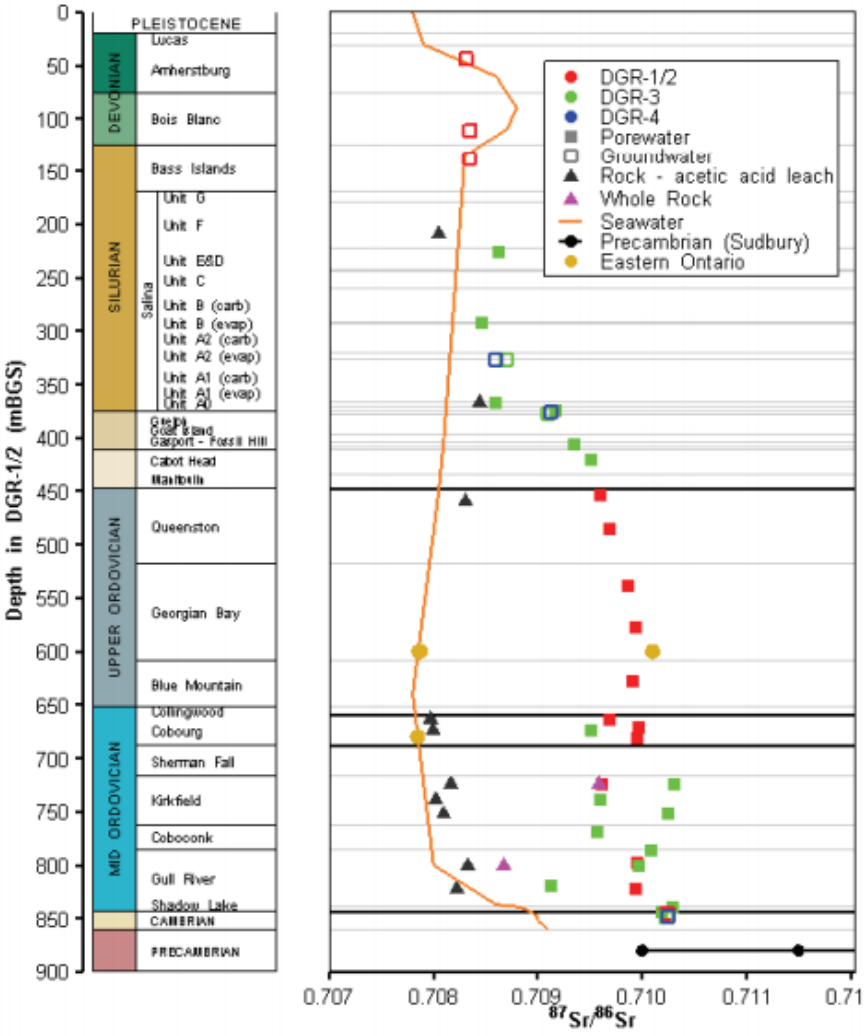

Figure 1.1: Strontium isotopes profile in DGR, for groundwaters, porewaters and rocks with seawater strontium isotopes curve from Veizer (1999). Precambrian values from Sudbury (Frape, Fritz, & McNutt, 1984) (Raven, et al., 2011).

Different hypotheses have been brought up to explain such a difference in strontium isotopes ratios between rocks and porewaters. The rock could have been leached by porewaters over time, resulting in ion-exchange between the two phases.

However, strontium isotope ratios of porewaters from the upper Ordovician in Figure 1.1 show a regular pattern that is not typical for leached rocks. That process would lead to an $^{87}Sr/^{86}Sr$ value similar to that of the rock. That led to another possibility to explain the difference in $^{87}Sr/^{86}Sr$ ratios: β-decay of ^{87}Rb over time in residual porewaters and/or in the rock, causing a steady increase of ^{87}Sr that can be recovered from the porewater. As the radionuclide is a monovalent cation, it does not behave the same way as strontium does. Once decayed in the rock, strontium may be excluded from the original mineral as it is not compatible, and would end up in the porewater. The decay being correlated with time, it could be possible to create the regular pattern observed in Figure 1.1 if no other sources of strontium or rubidium has mixed with porewaters. Finally, it is plausible that none of these processes take place in this system, and the ingrowth of ^{87}Sr is simply attributed to ^{87}Rb decay present in porewaters themselves.

1.2 Objectives

The overall objective of this project is (1) to determine the origin of the porewater and (2) to explain the difference in isotopic signature of strontium in rocks and in porewaters for the Upper Ordovician shales. Chosen samples of porewaters were analyzed for strontium and rubidium isotopes. Corresponding rock samples were sequentially leached to discriminate strontium and rubidium isotopes from the different minerals. Data collected lead to a better understanding of the process in which the porewaters became enriched in ^{87}Sr and were used (3) to determine the age of the rocks and porewaters.

2.0 LITERATURE REVIEW

2.1 Study area

2.1.1 Location and topography

The area under study is located in southern Ontario, next to the Lake Huron, on the Bruce Nuclear Power Plant site (Figure 2.1).

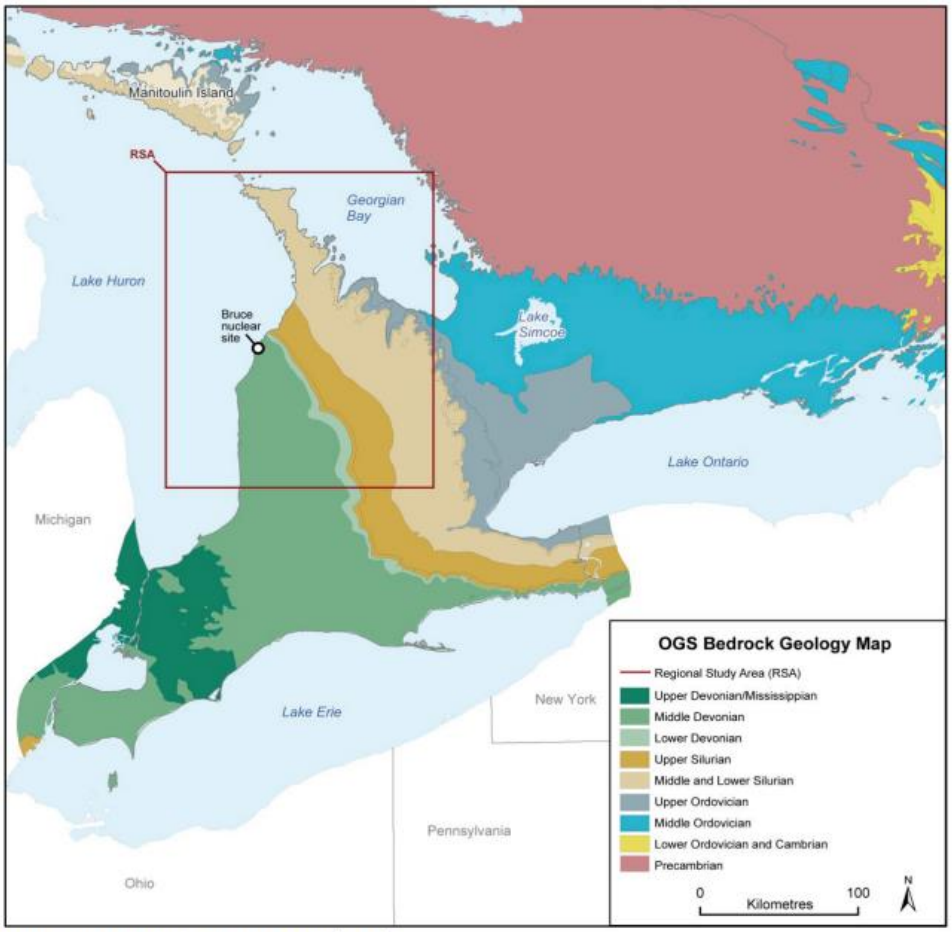

Note: After Ontario Geological Survey (1991).

Figure 2.1: Bedrock geology of southern Ontario and regional site area (Raven, et al., 2011)

Several boreholes were drilled on the Bruce Nuclear site, as shown in Figure 2.2. Many parameters were measured from these cores, in order to collect more information

on the feasibility of the project. In this thesis study, cores DGR-5 and DGR-6 were emphasized.

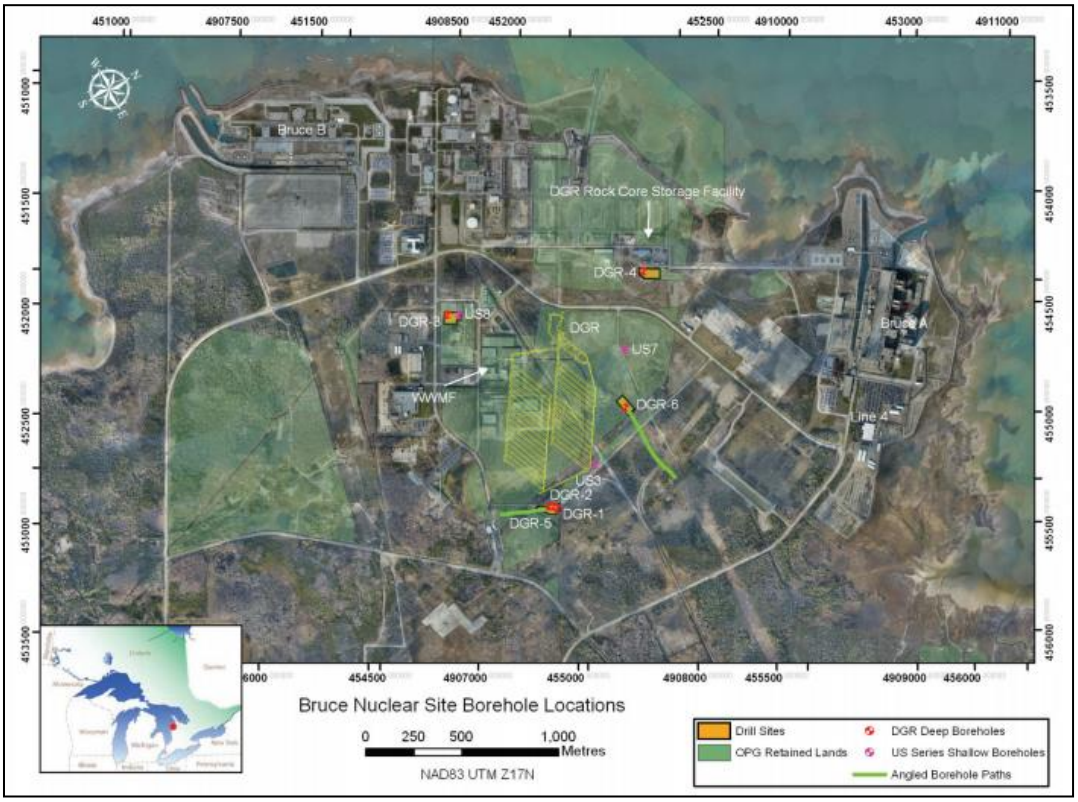

Figure 2.2: Bruce nuclear site borehole locations (Raven, et al., 2011)

2.1.2 History of southern Ontario

The Ordovician rocks were formed during the Paleozoic Era, spanning from 541 to 252 million years before present. The Ordovician period covers the time between 485 and 443 million years before present. The beginning and the end of the period correspond with major extinction events. At this time, the present eastern North America was located in the tropics and was covered by inland seas. As a result, the southern Ontario Paleozoic bedrock was formed by deposited marine sediments, from the Cambrian to the early Carboniferous period (324 million years ago) (Armstrong & Carter, 2010).

2.1.3 Ordovician carbonates

The Ordovician carbonates, located in the middle Ordovician layers, are subdivided into 2 groups: the Black River Group, which includes the Shadow Lake, Gull River and Coboconk Formations, and the Trenton Group, which includes the Kirkfield, Sherman Fall, Cobourg, and Collingwood Formations (Armstrong & Carter, 2010). These rocks were formed during a major regional marine transgression that occurred after the uplift and erosion of the Cambrian rocks. The transgression caused the overall sequence of supratidal and tidal flat clastic/carbonates to lagoonal/shoal and deep shelf carbonates (Kobluk & Brookfield, 1982). As this study focuses on the upper part of the middle Ordovician, only the Cobourg Formation (Lower Member of the Lindsay Formation) and the Collingwood Member (Lindsay Formation), both part of the Trenton Group, will be described.

The Cobourg Formation is made of blue-grey to grey-brown fossiliferous limestones and argillaceous limestones, with rocks ranging from very fine- to coarse-grained (Armstrong & Carter, 2010). The Collingwood Member is formed of dark grey and black calcareous shales, rich in organic carbon, overlying the fine-grained nodular limestones of the Cobourg Formation (Armstrong & Carter, 2010). Mineralogical analysis showed it is actually made of impure limestone or lime marlstone with high-organics contents, causing its dark color (Macauley, Fowler, Goodarzi, Snowdon, & Stasiuk, 1990).

2.1.4 Ordovician shales

The upper part of the Ordovician consists of orogeny-derived marine clastic sediments (shale), deposited after the inundation of the Trenton Group. The area was

flooded after the carbonate platform of the Trenton Group collapsed, at the beginning of the Taconic Orogeny. The resulting rocks are divided between 3 different formations: Blue Mountain, Georgian Bay, and Queenston.

The Blue Mountain Formation is characterized by blue-grey to grey-brown shales with variable amounts of siltstone, sandstone and limestone interbeds. The Georgian Bay Formation is very similar, but has more greenish- to bluish-grey shale and contains more fossils. Because of their similarities, the two formations are often combined and named together. On the other hand, the 275-metre thick Queenston formation is characterized by shale varying from red to maroon, with amounts of green shale, siltstone and sandstone and limestone (Donaldson, 1989). The top of the formation shows a discontinuity caused by a drastic sea level drop. This marine transgression caused the return of the carbonate-forming conditions, in which the lower Silurian units formed (Manitoulin, Cabot Head, Fossil Hill, Lions Head, Gasport, Goat Island and Guelph Formations).

2.1.5 Silurian units

The lower Silurian consists of intervals of sandstone, shale and limestone, formed by the marine transgression previously explained. The upper section is characterized by carbonate deposition, evaporites and related sediments (Armstrong & Carter, 2010). The difference in composition is an indication of changes in the marine and sedimentary environments. In facts, the Silurian rocks are the result of rapid basin subsistence and arch uplift caused by the late Silurian Acadian Orogeny. The Michigan Basin became more and more restricted, leading to evaporation of the water and precipitation of carbonate, gypsum, anhydrite, halite and sylvite (Raven, et al., 2011). Occasional

intrusions of fresh marine water caused the repeating pattern of carbonates, evaporites and argillaceous sediments observed in the Upper Silurian strata.

2.2 Strontium and rubidium dynamics

Isotopic systems are commonly used in geochronology and as tracers. The large variety of radioisotopes allows dating objects from a few days to billions of years old, making isotope systems powerful tools for scientists. Combined with stable isotopes, they provide clues on past climates, origins of pollutants, and mixing rates of waters.

Strontium is the 16th most abundant element in Earth's crust, with a crustal abundance of 370 ppm (Lide, 2005). It is a soft metal that substitutes for calcium in numerous minerals such as apatite, gypsum, anorthite and carbonates, as they are both divalent cations and have similar ionic radii (1.32 Å for Sr^{2+}, 1.14 Å for Ca^{2+}). In minerals in which Si^{4+} is replaced by Al^{3+}, Sr^{2+} can substitute for K^{+}, like in smectite and vermiculite. The same process takes place in K-bearing minerals with rubidium and potassium, as the elements are both monovalent and have similar ionic radii (1.66 Å for Rb^{+}, 1.52 Å for K^{+}) (Shannon, 1976). It is the case in muscovite, illite, and alkali feldspars, for example (Capo, Stewart, & Chadwick, 1998). Their different valences also have an impact on the hydrated radius on both ions. Because strontium is divalent, it will attract more water molecules than rubidium, and thus be larger. The hydrated radii are estimated to 2.28 Å for rubidium and 4.12 Å for strontium respectively (Ganguly, 2012).

Strontium and rubidium isotopes are widely used to identify geological processes such as continental weathering and tectonic activity. Four stable strontium isotopes occur in nature: ^{84}Sr (0.56%), ^{86}Sr (9.86%), ^{87}Sr (7.00%) and ^{88}Sr (82.58%). From these four, only ^{87}Sr is radiogenic. It is a product of the radioactive β-decay of ^{87}Rb (Capo, Stewart,

& Chadwick, 1998) described in Equation 2.1 (Veizer, 1989). Rubidium has 2 isotopes: ^{85}Rb (72.17%) and ^{87}Rb (27.83%), the latter being the only radioactive species, with a very long half-life of 4.88x10^{10} years. ^{87}Sr is commonly referred to as the "daughter", and ^{87}Rb, the "parent".

$$^{87}Rb \rightarrow {}^{87}Sr + \beta^{-} + \bar{\upsilon} + Q \qquad \text{Equation 2.1}$$

2.2.1 Isotope fundamentals

Most isotopes are expressed as a relative atomic ratio to the most abundant isotope for each element. They are usually measured with respect to references of a known isotopic content. For example, ^{18}O/^{16}O is expressed in comparison to Vienna Standard Mean Ocean Water (VSMOW) for water samples and to Vienna Pee Dee Belemnite (VPDB) for carbonates. The dimensionless ratio, called delta (δ), is expressed in parts per thousand, or permil (‰) and is calculated according to Equation 2.2 (Clark & Fritz, 1997):

$$\delta\ (‰) = \left(\frac{R_{sample}}{R_{standard}} - 1\right) * 1000 \qquad \text{Equation 2.2}$$

where R_{sample} and $R_{standard}$ are the atomic ratios in the sample and reference material.

In the case of strontium isotopes, it is possible to use the same notation as described above, as in Equation 2.3.

$$\delta^{87}Sr = \left(\frac{\left[{}^{87}Sr/{}^{86}Sr \right]_{sample}}{\left[{}^{87}Sr/{}^{86}Sr \right]_{standard}} - 1 \right) * 1000 \qquad \text{Equation 2.3}$$

In this specific case, absolute strontium isotope ratios can be measured directly with new technologies, without using the delta notation. The international reference NIST SRM-987 ($^{87}Sr/^{86}Sr = 0.71025$) is used to calibrate instruments in this situation. As a result, in most publications, strontium isotopes are expressed in absolute ratios rather than with the δ notation.

2.2.2 Strontium cycle

Depending on their nature, rocks may contain high levels of strontium. Sr is released from rocks by weathering and erosion processes, including actions from winds, animals and plants. Water is the main vector for Sr to reach rivers, lake, and eventually oceans – the largest reservoir of dissolved Sr – and to be deposited in marine carbonates. Tectonic activity and volcanism are then responsible for recycling crustal material. Isotopic signatures of strontium may be different from one reservoir to another, as shown in Figure 2.3.

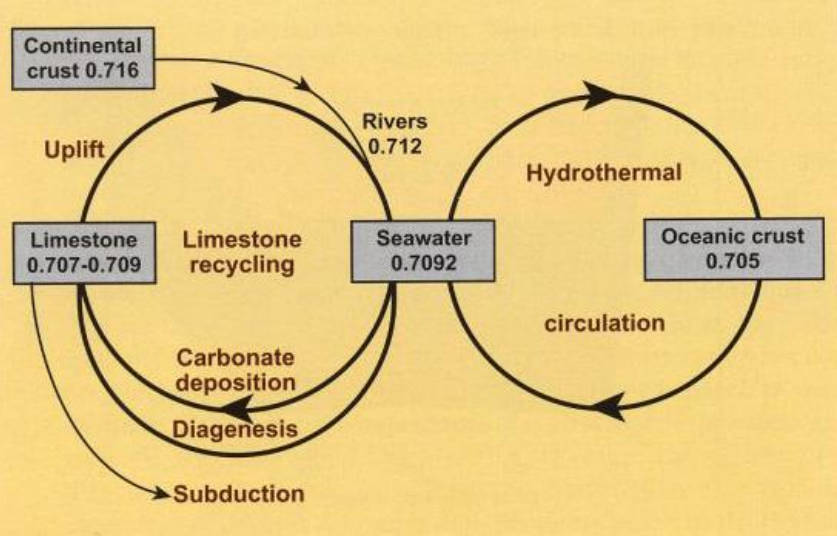

Figure 2.3: Strontium fluxes and $^{87}Sr/^{86}Sr$ in reservoirs (Hodell, Mead, & Mueller, 1990)

Alterations of isotopic signatures cannot be explained by isotopic fractionation in a sedimentary basin system, as it is unlikely to happen. The mass difference between the different isotopes is too low (^{87}Sr is only 1.1% heavier than ^{86}Sr) for physical and chemical processes to use one preferentially. However, interactions between rock and water may change the ratio, depending on the mineralogy. For example, a clay mineral containing high levels of Rb will undergo ^{87}Rb decay over time, thus the $^{87}Sr/^{86}Sr$ ratio in the clay mineral will rise. Water-rock interactions could then be responsible for an increase of the $^{87}Sr/^{86}Sr$ in the water. On the other hand, the strontium isotopes ratio in a carbonate mineral containing very low levels of Rb^{+} will not get significantly altered over time.

In the case of sedimentary rocks deposited in marine environment, rocks and porewaters have the same $^{87}Sr/^{86}Sr$ ratio as the seawater at the time of deposition (Faure & Gunter, 1991). A higher ratio measured in the water could indicate some mixing with an external source of rubidium or enriched strontium. It is then possible to conclude that

Sr isotopes ratios in the different reservoirs are mainly altered by the presence of ^{87}Rb, which decays over time, and by mixing with sources of different ratios.

In oceans, the residence time of Sr is between 2 and 4 million years (Hodell, Mead, & Mueller, 1990), which is much longer than the oceanic mixing rate of a few thousand years (Veizer J. , 1992). This explains why strontium concentration is relatively uniform in oceans.

2.2.3 Rubidium cycle

Because of its very large radius, rubidium is excluded from crystals when magma cools down. Being sequentially excluded, late-stage magmatic products tend to be highly concentrated in rubidium (Anderson, 1989). Examples are pegmatite, biotite and muscovite, which could contain more than 1000 ppm of rubidium. As a result, Rb is present in greater concentration in crustal material than in mantle minerals, with which it is virtually incompatible. Therefore, weathering products from the crust are enriched in ^{87}Rb and become more radiogenic over time, leading to greater values of $^{87}Sr/^{86}Sr$. This corresponds to the high strontium isotopes ratio shown in Figure 2.3.

Rubidium moves between rocks and water the same way strontium does. However, it rarely forms actual minerals. It is adsorbed onto clay minerals such as illites more strongly than K^+. Of course, its size and valence will not allow it to be incorporated in minerals such as carbonates like strontium does. Rubidium substitutes for potassium in minerals such as orthoclase and biotite.

The chemistry of strontium and rubidium, as previously explained, is responsible for various concentrations of these two elements in the different reservoirs and types of rocks, as shown in Table 2.1.

Table 2.1: Average concentrations of calcium, strontium, potassium and rubidium in different reservoirs.

	Ca (ppm)	Sr (ppm)	K (ppm)	Rb (ppm)	Reference
Average crust	41 000	370	21 000	90	(Sposito, 1989)
Modern Sea Water	414 000	7 620	425 000	110	(Holland, 1984)
Deep-Sea Carbonate	312 400	2 000	2 900	10	(Faure G. , 1986)
Carbonate	302 300	610	2 700	3	
Shale	22 100	300	26 600	140	
Deep-Sea Clay	29 000	180	25 000	110	

2.2.4 Rb-Sr dating

Because ^{87}Rb is radioactive, it can be used, combined with its daughter ^{87}Sr, to date minerals. With a constant of $(1.3968 \pm 0.0027)x10^{-11}$ decay per year (Rotenberg, Davis, Amelin, Ghosh, & Bergquist, 2012), this isotopic system could technically be used to date material older than the age of the universe, $13.77x10^{9}$ years old (National Aeronautics and Space Administration, 2012). The rate of decay is directly proportional to the number of atoms, expressed by:

$$\frac{dN}{dt} \propto N$$

where N is the amount of radioactive parent isotope. Because the amount of parent isotope is constantly diminishing, dN/dt has a negative value. The decay constant, λ, also has to be considered to establish the number of decays:

$$\frac{dN}{dt} = -\lambda N$$

By rearranging and integrating the previous equation:

$$\int_{N_o}^{N} \frac{dN}{N} = -\lambda \int_{t_0}^{t} dt$$

$$ln\left(\frac{N}{N_0}\right) = -\lambda(t - t_0)$$

Replacing t_0 by its real value (0), we obtain the following equation:

$$\boldsymbol{N = N_0 e^{-\lambda t}} \qquad \text{Equation 2.4}$$

where N is the amount of radioactive parent isotope at time *t*, N_0 is the initial amount of radioactive parent isotope, t is the elapsed time, and λ is the decay constant. The amount of daughter isotopes, D, is then expressed by the difference between N_0 and N:

$$\boldsymbol{D = N_0 - N} \qquad \text{Equation 2.5}$$

Thus, by replacing N in Equation 2.5 by rearranged Equation 2.4, it is possible to get a formula that directly leads to the amount of daughter isotope from decay:

$$\boldsymbol{D = N_0 - N = Ne^{\lambda t} - N = N(e^{\lambda t} - 1)} \qquad \text{Equation 2.6}$$

This last equation is considered true in a case where no daughter isotope is found initially. When it is not the case, the initial amount of daughter isotope, D_0, has to be taken into consideration in calculation.

$$\boldsymbol{D = D_0 + N(e^{\lambda t} - 1)} \qquad \text{Equation 2.7}$$

When applied to the Rb-Sr dating method, Equation 2.7 becomes Equation 2.8:

$$\left(\frac{^{87}Sr}{^{86}Sr}\right)_{total} = \left(\frac{^{87}Sr}{^{86}Sr}\right)_{initial} + \left(\frac{^{87}Rb}{^{86}Sr}\right)\left(e^{\lambda t} - 1\right) \qquad \text{Equation 2.8}$$

Because it is impossible to measure D_0, it has to be calculated from a graph, where it corresponds to the intercept (Figure 2.4). In the case of a sedimentary basin, this will likely correspond to the isotopes ratio of the seawater at the time of deposition (Chaudhuri & Clauer, 1992). From Equation 2.8, the age can be calculated by reporting the analytical value of $^{87}Sr/^{86}Sr$ on the Y-axis and $^{87}Rb/^{86}Sr$ on the X-axis for different components of the same material in an isochron, as shown in Figure 2.4. Knowing the value of the slope, it is possible to solve for t, which corresponds to the age of the material.

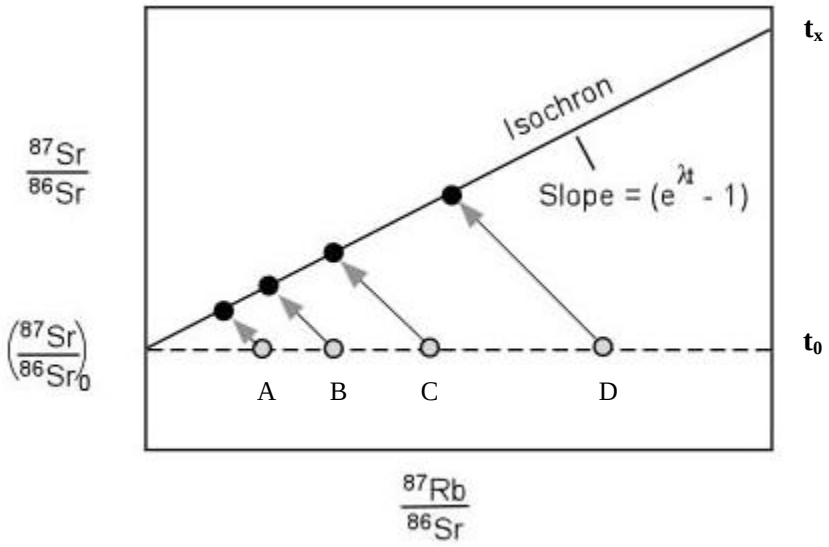

Figure 2.4: Rb-Sr isochron (Nelson, 2013)

From Figure 2.4, it is evident that the amount of ^{87}Sr at the time of measurement depends on the original content in rubidium. Therefore, knots A, B, C and D represent different components of a rock: calcite, whole rock, K-feldspar and biotite, for example,

with increasing Rb original content. Of course, this situation represents a case where no other sources of rubidium or strontium have mixed with the system. The main criterion in geochronology is that the studied system was closed since its formation, therefore there was no gain or loss of neither parent nor daughter isotopes by external sources or by diffusion. Also, the different minerals taken from the rock to build the isochron must have been formed and deposited at the same time. The minerals must have formed in chemical equilibrium one to another in order to make a trustable isochron.

2.2.5 Evolution of $^{87}Sr/^{86}Sr$ over geological time

Modern seawater has an $^{87}Sr/^{86}Sr$ value of 0.7090, which represents a mixture of both depleted oceanic (0.705) and continental enriched crust (>0.710) (Figure 2.3). The original bulk Earth's value of 0.69899 is directly derived from meteorites (Papanastassiou, Wasserburg, & Burnett, 1969). It is also referred to as the basaltic achondrite best initial ratio (BABI). The mantle's ratio has continuously been increasing over time, as ^{87}Rb is constantly decaying into ^{87}Sr (see Figure 2.5). After the crustal formation, the curve for the mantle became depleted in rubidium since the ion is concentrated in the crust. As mentioned in section 2.2.3, rubidium is excluded from minerals when magma cools down, enriching crustal rocks. This phenomenon is responsible for the steep curve of the crust, and depletion of the Rb/Sr ratio in the mantle in Figure 2.5. When a modern melt is derived from partial melting of the mantle, its $^{87}Sr/^{86}Sr$ value is lower than a melt from crustal rocks would be.

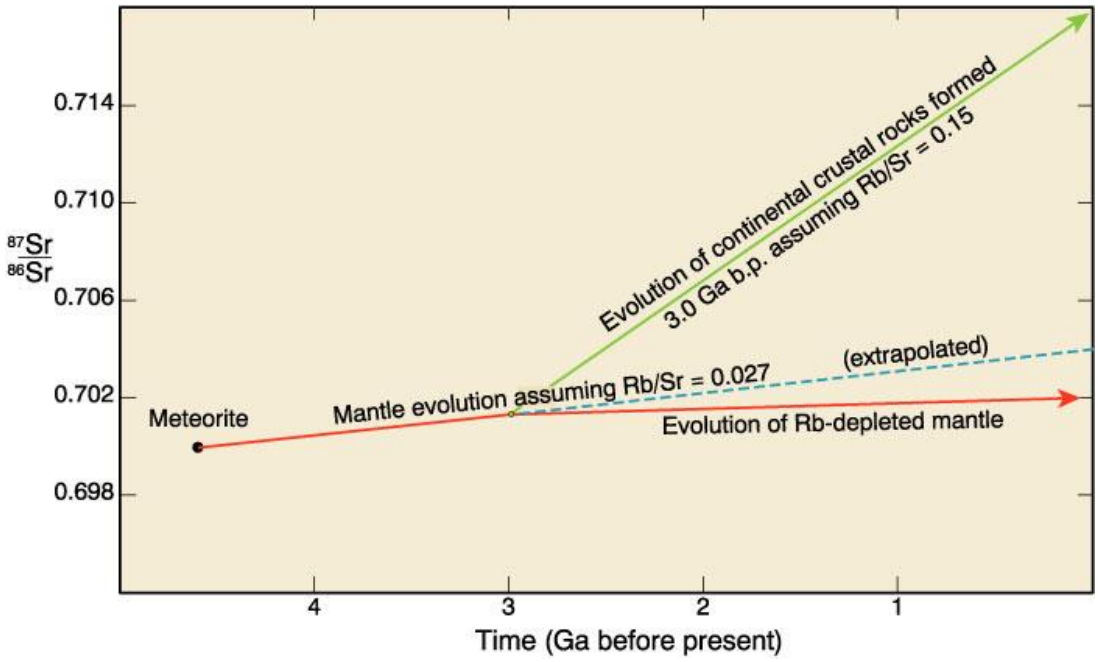

Figure 2.5: Estimated evolution of $^{87}Sr/^{86}Sr$ of the Earth's upper mantle, assuming a large-scale melting event producing granitic-type continental rocks at 3.0 Ga b.p. (Wilson, 1989)

Modern values of strontium isotopes ratios are not as linear as in Figure 2.5. They are controlled by different geological processes. Figure 2.6 shows variations of $^{87}Sr/^{86}Sr$ ratio in seawater throughout Phanerozoic Time. Those variations have been explained by high volcanism and spreading ridges, causing the release in oceans of ^{87}Sr-depleted magmas. On the other hand, increases in ^{87}Sr are usually caused by weathering of continent by glaciers, as observed in the late Cenozoic sediments (Clark & Fritz, 1997).

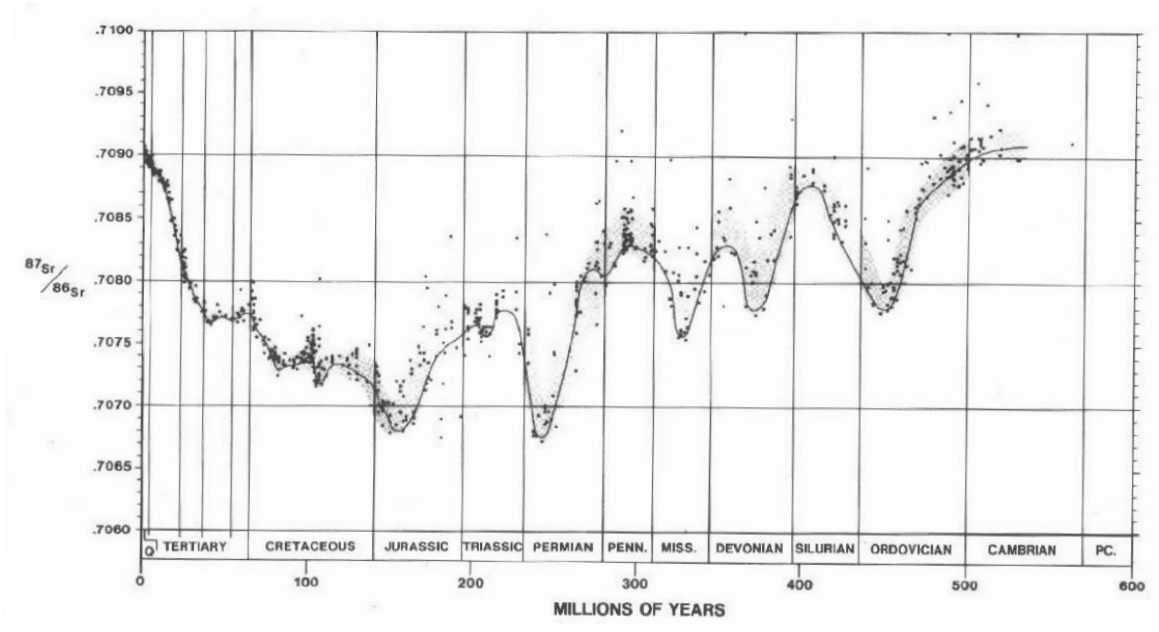

Figure 2.6: Strontium isotopes in seawater through time (Burke, et al., 1982)

Geochemistry of elements is also considered to explain variations of $^{87}Sr/^{86}Sr$ in groundwaters, rivers and lakes, as the ratio is directly linked to the composition of terrains. ^{87}Sr being the daughter of ^{87}Rb, the ratio will be directly linked to the potassium content, which is high in clays and low in limestone once the water has reached equilibrium with the rock. Thus, waters sitting on different terrains may have significantly different isotopic signatures.

2.3 Mineral dissolution

Samples selected for this study are located just above the proposed repository, which is 680 m deep (Figure 2.7). Emphasis was put on rocks from the upper and the top of the middle Ordovician layers, including Queenston, Georgian Bay, Blue Mountains, Collingwood and Cobourg formations, as the divergence between the Sr isotopes ratio in rocks and porewaters happens mainly in these layers (ref. Figure 1.1). Shale and

argillaceous limestone are the main type of rocks found in the upper and middle Ordovician, respectively.

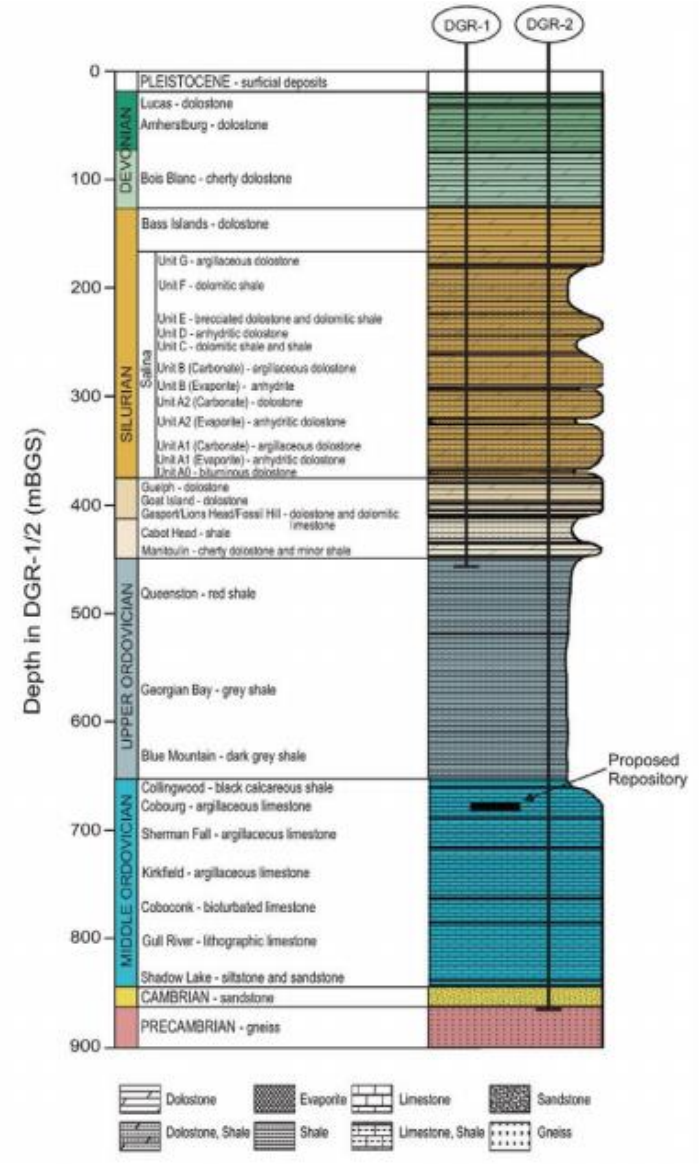

Figure 2.7: Stratigraphy of the Bruce nuclear site (Raven, et al., 2011)

Major components of the rock were previously identified with various techniques (electron microprobe, XRD, SEM/EDS, lithogeochemistry) (Raven, et al., 2011). Results are shown in Figure 2.8.

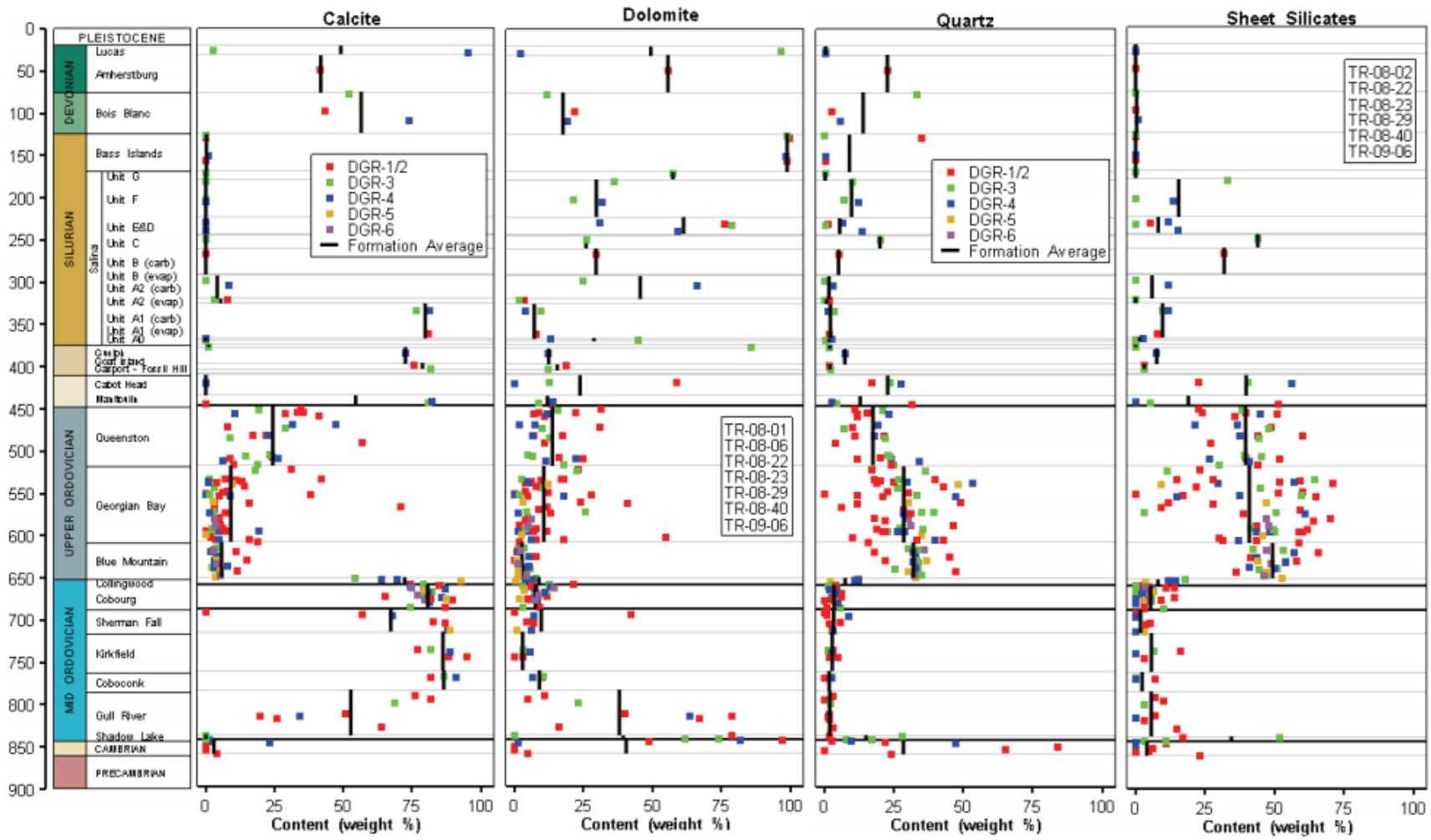

Figure 2.8: Content weight of major components (Raven, et al., 2011)

Knowing the composition of the rocks was essential to determine the procedure to be used to dissolve specific minerals. Based on Figure 2.8, the main components (calcite, dolomite, and silicates) were targeted in the dissolution sequence, as they are found in various concentrations at the studied depths. This choice of sequence is also consistent with the site history. Calcite has been deposited at the bottom of the sea along with clay minerals that likely were brought by erosion of the continent. Later on, Silurian brines have infiltrated the rocks, causing dolomitization. Since the three mineral phases have a different history and mechanism of formation, it was sensible to separate them.

Whole-rock dissolution is a widely used technique around the world to determine mineral content and isotopes. Several research groups have dissolved carbonate rocks in order to get strontium isotopes ratios. By doing so, it is possible to extract strontium from every phase and have a better understanding of interactions between them. Different leaching sequences have been tried to separate calcite from dolomite and silicates. The main idea is to dissolve the entire sample in a specific sequence:

- Remove labile, adsorbed ions, and water soluble evaporites;
- Dissolve calcite;
- Dissolve dolomite and other carbonates;
- Dissolve silicates.

The removal of labile and exchangeable ions is necessary in order to avoid contamination of the Sr ratio in further leachates. Ammonium acetate solution (1M) is commonly used to do this (Jacobson, Blum, Page Chamberlain, Poage, & Sloan, 2002). However, ammonium acetate is known to form complexes with calcium, which may

cause some calcite dissolution (Bailey, McArthur, Prince, & Thirlwall, 2000). Deionized water happens to be an appropriate alternative to avoid this problem (Gosselin, Harvey, Frost, Stotler, & Macfarlane, 2004).

Calcite dissolution can be achieved by leaching with acetic acid (Tessier, Campbell, & Bisson, 1979) (Lerouge, et al., 2010). A rapid leach with low-concentration acetic acid – usually 5 to 10% – is proven to maximize dissolution of calcite over dolomite (Sharp, Creaser, & Skidmore, 2002).

Treatment with HCl is common when it comes to dissolve all types of carbonates. However, hydrochloric acid will also remove a significant amount of Sr from the surface of clay particles without dissolving any of the silicate phases (Clauer, Chaudhuri, Kralik, & Bonnot-Courtois, 1993). HCl also attacks hydrated oxides, sulfides and phosphates (Gosselin, Harvey, Frost, Stotler, & Macfarlane, 2004).

The final step includes dissolution of the remaining silicates. Most of the time, a mixture of nitric, hydrofluoric and perchloric acid is used (Jacobson, Blum, Page Chamberlain, Poage, & Sloan, 2002) (Sharp, Creaser, & Skidmore, 2002).

2.4 Previous work on the DGR cores

2.4.1 Porewater solutes extraction

Porewaters were extracted in 2008 using the crush and leach technique. After being crushed to 2-4 mm grain size, samples were heated to 150°C under vacuum to extract porewaters. This was followed by a deionized water leach of the same crushed rocks, for 60 days, in order to recover ions from porewaters. The resulting extraction factors are shown in racted under vacuum.

Table 2.2. An aliquot of the leaching water was then taken up for geochemical analyses. Original ion concentrations in porewaters were calculated by dividing the mass of ion in the leachate by the mass of porewater extracted under vacuum.

Table 2.2: Extraction factors for porewaters

Sample ID	Mass of porewater extracted (g)	Mass of water added for leaching (g)	Extraction factor
DGR5-497.50	1.5186	29.9841	19.74
DGR5-514.22	1.2865	32.2265	25.05
DGR5-525.57	1.2441	36.0370	28.97
DGR5-557.65	1.6867	32.3357	19.17
DGR5-564.96	0.7955	38.8617	48.85
DGR5-598.37	1.4268	35.3841	24.80
DGR5-625.23	1.4625	33.0629	22.61
DGR5-649.57	1.6137	32.6206	20.21
DGR6-654.12	1.4873	36.5946	24.60
DGR6-661.83	1.2537	37.9262	30.25
DGR6-662.17	0.6324	37.2685	58.93
DGR6-662.82	1.3021	36.9034	28.34
DGR5-671.30	1.3404	34.6608	25.86
DGR6-683.25	1.2299	36.7836	29.91
DGR5-683.57	1.0652	38.2880	35.94
DGR5-697.85	1.1594	35.6760	30.77
DGR6-697.97	1.4332	37.0231	25.83
DGR5-715.60	1.3173	37.8426	28.73
DGR5-724.90	2.7652	39.5468	14.78
DGR5-731.02	2.0117	36.8032	18.30
DGR5-734.06	1.0753	35.1175	32.66

2.4.2 Preliminary analyses

Some preliminary strontium isotopes analyses were done a few samples from the upper Ordovician shale and middle Ordovician limestone, in 2010. Once porewaters were extracted and ions were leached, a few grams of rocks were rinsed with deionized and

dried before being crushed to powders and leached with 5% acetic acid, for 20 minutes, in an ultrasonic bath, to dissolve calcite. In addition, 2 samples from the upper Ordovician and 2 samples from the middle Ordovician were rinsed, dried, and completely dissolved to analyze the whole rock strontium isotopes ratio. Results are shown in Figure 2.9.

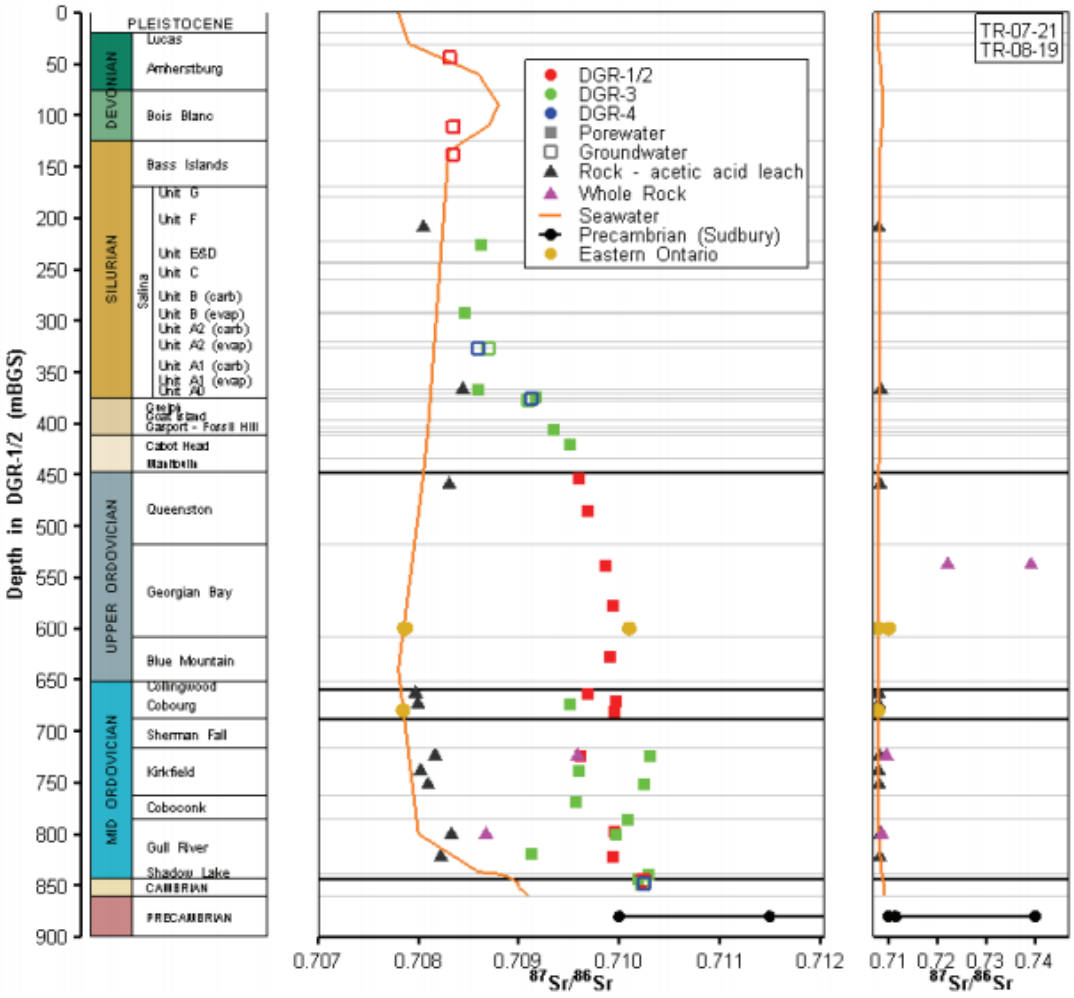

Figure 2.9: Strontium isotopes in groundwater, porewater and rocks (Raven, et al., 2011)

Acetic acid leachates (black triangles) from the upper and middle Ordovician show strontium isotopes ratios falling close to the seawater line, indicating carbonates likely originate from the seawater. Whole rock values (purple triangles) are more

enriched in shales than in limestones, which is expected as they contain more clay minerals.

Porewater values from the shales show enrichment in ^{87}Sr that neither is in equilibrium with carbonate phases (acetic acid leachable) nor it is with whole-rocks values. This quick analysis suggests that simple leaching of the rocks by pore fluids cannot be a valid explanation for the enrichment of radiogenic strontium in porewaters.

3.0 METHODOLOGIES

3.1 Sample selection

The focus of this study was put on DGR 5 and 6 cores, more specifically in the upper Ordovician shales and the Cobourg formations. Table 3.1 shows samples used for the project with respect to their formation and depth. All available samples were picked for further analyses. Formations and depths relative to DGR-1/2 are shown in Figure 3.1. Results will later be expressed relative to DGR-1/2.

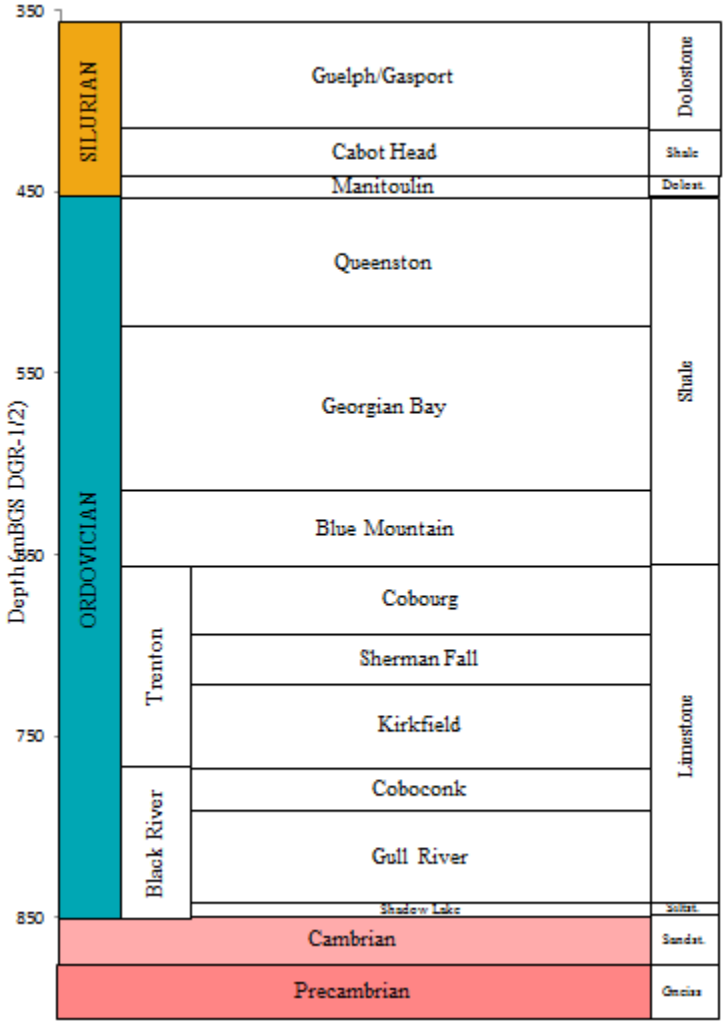

Figure 3.1: Formations and depths relative to DGR-1/2

Table 3.1: Samples availabilities and associated formations

Formation	Core	Depth (mLBGS)	Actual Depth (mBGS)[1]	Depth relative to DGR 1/2	Rock sample	Porewater sample
Queenston	DGR5	497.50	456.52	458.01	√	√
Queenston	DGR5	514.22	472.36	473.82		√
Queenston	DGR5	525.57	483.14	484.59	√	√
Queenston	DGR5	557.65	513.72	515.12		√
Georgian Bay	DGR5	564.96	520.69	522.20	√	√
Georgian Bay	DGR5	598.37	552.59	554.92	√	√
Georgian Bay	DGR5	625.23	578.28	581.28	√	√
Georgian Bay	DGR5	649.51	601.56	605.17		√
Georgian Bay	DGR6	654.12	571.89	582.42		√
Georgian Bay	DGR6	661.83	578.67	589.11		√
Georgian Bay	DGR6	662.17	579.21	589.41	√	√
Georgian Bay	DGR6	662.82	578.38	589.98		√
Blue Mountain	DGR5	671.30	622.55	625.33		√
Georgian Bay	DGR6	683.25	596.39	607.67		√
Blue Mountain	DGR5	683.57	634.43	636.57		√
Blue Mountain	DGR6	697.79	608.60	619.36		√
Blue Mountain	DGR5	697.85	648.30	649.71		√
Cobourg	DGR5	715.60	665.60	666.57	√	√
Cobourg	DGR5	719.91	669.81	671.01	√	
Cobourg	DGR5	724.90	674.68	676.15		√
Cobourg	DGR5	731.02	680.65	682.45	√	√
Cobourg	DGR5	734.06	683.61	685.58	√	√

[1] The difference between *depths* and *actual depths* is attributed to angle when cores were drilled (ref. Figure 2.2)

Porewaters were extracted in 2008 from crushed rocks (2-4 mm) as described in section 2.4.1 and stored in 15 mL plastic tubes until ready for analyses. Crushed rocks samples were left in deionized water and stored in 50 mL Falcon tubes. All samples were stored in cardboard boxes, kept away from heat and light until the beginning of this project in 2013.

3.2 Preparation

A few grams of the crushed rock samples were taken out of the Falcon tubes, rinsed with deionized water and dried at 70°C overnight. They were then taken to the crushing room to be pulverized to fine powders with the help of a disk mill. Between each sample, the equipment was rinsed with water, ethanol, and dried out. Silica beads were crushed in the disk mill in order to clean the pores before it was rinsed again with water, ethanol, dried, and pre-contaminated with the next sample. After being crushed, samples were stored in 15-mL plastic tubes until ready for analyses.

Rock and porewater samples were transported at the Isotope Geochemistry and Geochronology Research Centre (IGGRC) at Carleton University for strontium isotopes analysis. All laboratory work related to strontium isotopes took place in the IGGRC clean laboratory, using ultra clean Teflon containers and instruments.

In order to extract strontium from the different components of the rock, samples underwent sequential leaching based on information from section 2.3. The time of reaction and the amount of chemical required for each step was based on previous experiments done at the IGGRC. Selected chemical were nanopure water, 5% acetic acid, 6N HCl and a mixture of 50% HF-12N HNO_3. Various times of leaching were tried to find the optimal dissolution process in order to separate adsorbed ions, calcite, dolomite and silicates. A reference value was available to confirm the validity of the method: the strontium isotopes ratio for the acetic acid leachate of the DGR3-687.10 had to be of 0.7080, which corresponds to the seawater value (Spencer, 2013). Once this value was obtained for this sample, the method was applied on all other rock samples.

3.3 Analytical procedure

3.3.1 Rock samples

Powdered rock samples were weighted. Masses are indicated in Table 3.2. Samples were run by batches of 3 at the time, for logistic reasons. Each batch took 3 weeks to analyze for strontium isotopes. Only 100 mg of the first samples were used to compare the quality of the signal on the mass spectrometer used later on. Since the quality of the signal was much better when using 200 mg of samples, it was decided to keep this amount for other batches.

Table 3.2: Masses of rock samples

Sample ID	Mass (mg)
DGR5-497.50	100.17
DGR5-525.57	200.96
DGR5-564.96	199.59
DGR5-598.37	198.36
DGR5-625.23	199.97
DGR6-662.17	199.17
DGR5-715.60	201.87
DGR5-719.91	199.08
DGR5-731.02	201.12
DGR5-734.06	200.99

Samples were put in a 15 mL Teflon container with 3 mL of nanopure water, capped and left in an ultrasonic bath for 20 minutes before being taken out to rest for 5 minutes. The mixtures were transferred in tubes and were centrifuged for 4 minutes. Water supernatants were pipetted, transferred in pre-labelled 5 mL Teflon containers and stored. The remaining powders were mixed with 3 mL of 5% acetic acid, put back in their original Teflon containers and left in the ultrasonic bath for 20 minutes again. After being

taken out to rest for 5 minutes, the mixtures were transferred again in tubes to be centrifuged for 4 minutes. Acidic supernatants were extracted with pipettes, transferred in new pre-labelled 5 mL Teflon containers and stored. The remaining powders were mixed with 3 mL of 6N HCl and went through the same procedure again. After supernatants were removed and stored, the powders were entirely dissolved in a mixture of 50% HF - 12N HNO_3. Samples were capped and left on a hotplate at 140°C until complete dissolution.

After 6 days, the hot containers were uncapped and placed on the hotplate to evaporate to dryness. A few drops of 7N HNO_3 were added to the residues and evaporated, and then 3 mL of 6N HCl were added. The containers were capped and left on the hotplate overnight. On the following day, all 12 containers (4 per sample – one for each leachate) were opened and evaporated at 90 C. A few drops of 7N HNO_3 were added in all containers and dried down, and samples were redissolved in 3 mL of 2.5N HCl. All containers were capped and left on the hotplate at 90°C overnight.

On the following morning, samples were divided in 2 subsamples of 1.5 mL each. The first portion was dried, dissolved in 1.5 mL 7N HNO_3 and stored in clean 15 mL plastic tubes for further ICP analyses. The second subsample underwent strontium extraction, using Dowex 50-X8 Cation resin, following the procedure described in Appendix A. The strontium enriched phases were collected in clean pre-labelled Teflon containers, left on a hotplate at 90°C to dry overnight, and spotted with 7N HNO_3 again on the following day to remove all traces of organic molecules. All containers were capped and stored until ready for the next step.

Samples were then brought to the mass spectrometer laboratory. They were dissolved in 4.2 µL of concentrated H_3PO_4, and 3 µL of each were put on single tantalum filaments with a pipette and dried. An additional filament was prepared with NIST SRM-987 standard ($^{87}Sr/^{86}Sr = 0.710239 \pm 0.000014$) (Carleton University, 2012). Filaments were inserted on the carrousel and put in the thermal ionization mass spectrometer (TIMS). Samples were analyzed under vacuum on the following days. Table 3.3 shows analytical specifications of the instrument.

Table 3.3: Analytical parameters for the thermal ionization mass spectrometer

Brand	Fisher Scientific®
Filament	Single Tantalum
Current	2600-3000 mA
Temperature	1350-1400°C
Target signal	1.0 V
Number of measurements	100

Samples preserved for ICP analysis underwent proper dilution with 1% HNO_3 and were passed through 0.45 µm nitrocellulose filters. Cations (Na^+, K^+, Mg^{2+}, Ca^{2+} and Sr^{2+}) were measured by Inductively Coupled Plasma Optical Emission Spectroscopy (ICP-OES) using a Varian (Agilent)® Vista-Pro. Rubidium isotopes were determined by Inductively Coupled Plasma Mass Spectrometer (ICP-MS). Specifications for both instruments are shown in Table 3.4 and Table 3.5.

Table 3.4: Analytical parameters for the ICP-OES

Brand	Varian (Agilent) Vista Pro®
Detector	CCD
View	Radial
RF Power	1.35 kW
Plasma Gas Flow	15 L/min
Auxiliary Gas Flow	1.5 L/min
Carrier Gas Flow	0.8 L/min
Sample Uptake Rate	1.0 mL/min

Table 3.5: Analytical parameters for the ICP-MS

Brand	Agilent 7700x Quadrupole®
RF Power	1.50 kW
Plasma Gas Flow	15 L/min
Auxiliary Gas Flow	1.5 L/min
Carrier Gas Flow	1.0 L/min
Sample Uptake Rate	0.10 mL/min

3.3.2 Porewater samples

Porewater samples underwent proper dilutions with 1% HNO_3 and were analyzed for their content in sodium, potassium, magnesium, calcium and strontium with the ICP-OES. Analytical parameters are described in Table 3.4. Diluted samples were also run on the ICP-MS, with the analytical parameters described in Table 3.5. Appropriate standards were prepared as well for all ions.

Strontium isotopes were also measured in porewaters. To do so, 1.5 mL of each sample was dried down on a 90°C hotplate, in a clean Teflon beaker, at the IGGRC laboratory. Once dried, residues were spotted with 7N HNO_3 and dried again. 1.5 mL of 2.5N HCl was added to each beaker in order to perform strontium separation with Dowex 50-X8 cation exchange resin, as described in Appendix A. Strontium enriched phases were collected in pre-labelled clean Teflon containers, were dried on a 90°C hotplate, and

redissolved in 4.2 µL H_3PO_4. 3 µL of each samples were deposited on single tantalum filaments and dried. All samples along with a standard were put in the TIMS and analyzed on the following day. Analytical parameters are described in Table 3.3. A total of 21 porewater samples were analyzed (ref. Table 3.1).

3.4 Calculations

3.4.1 Strontium isotopes ratios

Strontium isotope ratios can be directly measured by thermal-ionization mass spectrometer. In fact, 2 ratios are measured: $^{88}Sr/^{86}Sr$, and $^{87}Sr/^{86}Sr$. The first one is called the *normalizing ratio*, as it should be constant in the environment. Neither ^{88}Sr nor ^{86}Sr are radioactive or radiogenic, so their ratio must be 8.375 in *any* sample. In parallel, the second ratio is measured. ^{87}Sr being radiogenic, the ratio varies from one sample to the other. When the instrument measures a value different than 8.375 for $^{88}Sr/^{86}Sr$, the software applies a correction factor over the $^{87}Sr/^{86}Sr$ value, to correct for the deviation. When measuring, filaments can reach a temperature of 1 400°C that can cause fractionation, explaining any deviation from the value. To ensure this factor is correct, a third ratio ($^{84}Sr/^{86}Sr$) is measured. Just like strontium 88 and 86, strontium 84 is constant in the environment, thus the expected $^{84}Sr/^{86}Sr$ ratio is 0.05649. The measured ratio multiplied by the correction factor should then always be equal to 0.05649.

The TIMS also corrects for the presence of ^{87}Rb, which causes interferences in the measurement of ^{87}Sr as both species have the same mass. If the concentration of rubidium is very low, it is possible for the detector to measure ^{85}Rb, to transform it into an $^{87}Rb/^{86}Sr$ ratio, and to substract this value from the measured $^{87}Sr/^{86}Sr$ ratio.

100 measurements are being taken of each sample. The software uses standard statistical parameters in order to calculate the actual values and uncertainties for each sample. Therefore, the arithmetic mean, standard deviation and standard error are calculated for each sample. Reported values for strontium isotopes ratios show the mean of these 100 measurements, and the uncertainty represents the standard error multiplied by 2. Since strontium isotope ratios are absolute measurements, no dilutions factors have to be taken in consideration.

3.4.2 Rubidium isotopes

Rubidium isotopes were measured with the ICP-MS, as mentioned previously. The appropriate standard solutions are prepared and a calibration curve is calculated. To avoid dealing with mass interferences between ^{87}Sr and ^{87}Rb, ^{85}Rb is measured and the concentration is back-calculated with the calibration curve. Since the abundance of each isotope is well known, ^{87}Rb could be determined by multiplying the concentration of ^{85}Rb by the abundance factor, which is 0.3856, as shown in Equation 3.1. In addition to that, the obtained result is multiplied by the dilution factor (DF) for both rocks and porewater samples. For porewaters, another factor has to be considered to get the original concentration of isotopes. When they were extracted, porewaters were diluted by factors shown in Table 2.2. This second factor, the extraction factor (EF) has to be applied on the calculated concentrations as well.

$$\left[^{87}\boldsymbol{Rb}\right]_{(\boldsymbol{ppm})} = \left(\frac{^{85}\boldsymbol{Rb}_{(\boldsymbol{counts})} - \boldsymbol{Intercept}}{\boldsymbol{Slope}}\right) * \mathbf{0.3856} * \boldsymbol{DF}(* \boldsymbol{EF}) \qquad \text{Equation 3.1}$$

3.4.3 Major ions

Major ions (sodium, potassium, magnesium, calcium) and strontium were measured by ICP-OES. Standard solutions are prepared and calibration curves are calculated for each analyzed ions. Just as for rubidium isotopes, ions concentrations are back-calculated with the calibration curves as described in Equation 3.2. The equation describes the calculation for sodium, but is applicable to the 4 other measured ions. Here again, the dilution factor (DF) must me applied for both rocks and porewaters. The extraction factors (EF) from Table 2.2 have to be considered as well in the case of porewaters.

$$[\boldsymbol{Na}]_{(\boldsymbol{ppm})} = \left(\frac{\boldsymbol{Na}_{(\boldsymbol{counts})} - \boldsymbol{Intercept}}{\boldsymbol{Slope}}\right) * \boldsymbol{DF}(* \boldsymbol{EF}) \qquad \text{Equation 3.2}$$

4.0 RESULTS AND DISCUSSION

4.1 Geochemistry

4.1.1 Rocks

Sodium, potassium, rubidium, calcium, magnesium, and strontium were analyzed to determine their amount in each sample, with the methodology described in 3.3. In rock samples, cations were expected to be representative of the lithology. Furthermore, they were used to determine the validity of the leaching sequence. Measurements were corrected for dilutions, and final concentrations are presented in

Table 4.1. For each element, concentrations are normalized for one kilogram of rock (ref. Table 3.2). Additionally, rubidium concentrations were calculated from ^{85}Rb measurements, as described in Section 3.4.2. Uncertainties are estimated to 1% for all concentrations.

Table 4.1: Concentrations of ions in rocks

	Sodium (mg/kg)				**Potassium (mg/kg)**				**Rubidium (mg/kg)**			
Sample ID	H_2O leachate	AcOH leachate	HCl leachate	HF/HNO_3 dissolution	H_2O leachate	AcOH leachate	HCl leachate	HF/HNO_3 dissolution	H_2O leachate	AcOH leachate	HCl leachate	HF/HNO_3 dissolution
DGR5-497.50	154	62.1	31.6	478	854	232	1 389	23 991	3.36	1.06	9.37	104
DGR5-525.57	124	70.1	54.3	544	540	550	1 250	19 481	1.49	0.89	6.92	133
DGR5-564.96	55.7	35.5	39.1	323	236	379	570	19 419	0.65	0.87	3.20	99.4
DGR5-598.37	108	44.2	29.8	101	355	467	713	13 065	1.28	0.88	5.52	30.3
DGR5-625.23	167	44.0	24.1	209	453	426	640	13 339	0.99	0.79	5.19	42.1
DGR6-662.17	27.4	48.3	47.2	1 105	103	297	435	15 002	0.68	0.52	2.48	80.3
DGR5-715.60	32.7	68.6	129	106	109	189	372	7 351	0.33	0.29	1.39	31.7
DGR5-719.91	28.3	47.6	94.0	65.7	85.4	129	227	5 049	0.27	0.24	1.13	24.7
DGR5-731.02	27.2	89.5	68.9	100	134	250	313	9 008	0.40	0.47	1.65	39.9
DGR5-734.06	35.2	49.6	56.9	55.7	93.0	129	193	5 161	0.28	0.26	1.07	20.1
	Magnesium (mg/kg)				**Calcium (mg/kg)**				**Strontium (mg/kg)**			
Sample ID	H_2O leachate	AcOH leachate	HCl leachate	HF/HNO_3 dissolution	H_2O leachate	AcOH leachate	HCl leachate	HF/HNO_3 dissolution	H_2O leachate	AcOH leachate	HCl leachate	HF/HNO_3 dissolution
DGR5-497.50	329	6 595	22 946	6 502	385	94 549	4 457	303	4.34	99.6	9.7	26.3
DGR5-525.57	77.9	939	6 129	6 695	765	94 396	42 940	2 636	5.16	134	29.4	22.7
DGR5-564.96	73.7	2 724	10 826	5 485	722	79 614	62 569	5 055	4.56	91.6	28.8	21.1
DGR5-598.37	143	1 404	2 612	1 398	327	14 784	28 280	335	3.32	65.6	15.0	7.46
DGR5-625.23	65.4	1 625	2 018	1 631	465	22 451	12 981	338	5.48	32.9	13.9	8.12
DGR6-662.17	25.5	802	7 777	4 397	245	129 498	64 060	4 648	1.66	213	65.0	24.7
DGR5-715.60	17.5	605	3 809	1 646	860	122 112	173 748	17 845	2.06	197	282	22.9
DGR5-719.91	21.7	637	3 729	1 262	1 190	129 636	175 246	14 787	2.62	181	253	17.1
DGR5-731.02	30.0	1 008	5 799	1 920	559	187 283	136 010	8 540	2.44	260	197	17.0
DGR5-734.06	24.6	797	2 803	1 024	1 741	175 815	160 419	10 853	2.84	223	219	13.3

As expected, concentrations in water leachates are very low compared to the other ones. This leach can be considered as a simple wash, but could also have dissolved cations adsorbed onto surfaces of clays and other minerals. Traces of celestite detected in those samples (Raven, et al., 2011) could also have been dissolved by the water leachate (Bailey, McArthur, Prince, & Thirlwall, 2000). Moreover, high concentrations of sodium in water leachates were measured in the upper part (DGR5-497.50 to DGR5-625.23). Those values are consistent with previous observations of halite in the upper Ordovician shales, with concentrations decreasing through depth (Jackson & Murphy, 2011).

The acetic acid and hydrochloric acid leachates are highly enriched in divalent cations. The purpose of doing both leaches was to preferentially dissolve calcite over other carbonates (mainly dolomite) with acetic acid, and to dissolve all of the other carbonates with HCl. Magnesium concentrations in both leachates lead to believe dolomite is concentrated in HCl, although small concentrations in AcOH show it might have been slightly affected by the acetic acid treatment. As expected, very high concentrations of calcium were measured, especially in limestones (DGR5-715.60 to DGR5-734.06). Calcium in both AcOH and HCl leachates are indicators of calcite, dolomite and ankerite, found in greater concentrations in limestones than in shales. It is not excluded that calcite was not entirely dissolved by acetic acid and partially ended up in the HCl leachate.

The first sample, DGR5-497.50, shows high concentrations of magnesium, which corresponds with high concentrations of dolomite found in mineralogical analyses. Magnesium and calcium concentrations are also not negligible in the HF/HNO_3 dissolutions, indicating their presence in clays. Anorthite, illite, chlorite and smectite,

which are all present in samples in various concentrations (Jackson & Murphy, 2011) are associated with these elements and could be responsible of their presence in the HF/HNO_3 solution.

Monovalent cations are found, in highest concentrations, in the final rocks dissolutions associated with clay minerals. Amongst the most abundant silicate minerals are illite, chlorite and smectite (Raven, et al., 2011), all rich in potassium and rubidium, since both cations have similar behaviours. Concentrations of potassium and rubidium are also consistent with the amount of sheet silicates found in samples (ref. Figure 2.8), as they follow the same trend. One sample (DGR6-662.17) shows especially high concentrations in sodium in the HF/HNO_3 solution. This observation is consistent with mineralogical analysis of these depths, showing high concentrations of albite.

The overall concentrations of measured cations are consistent with mineralogical analysis (ref. Figure 2.8) (Jackson & Murphy, 2011). The different concentrations are visually represented in Figure 4.1and Figure 4.2. Rubidium and potassium are following a similar trend when comparing their concentrations in the HF solution. The same observation can be made with calcium and strontium.

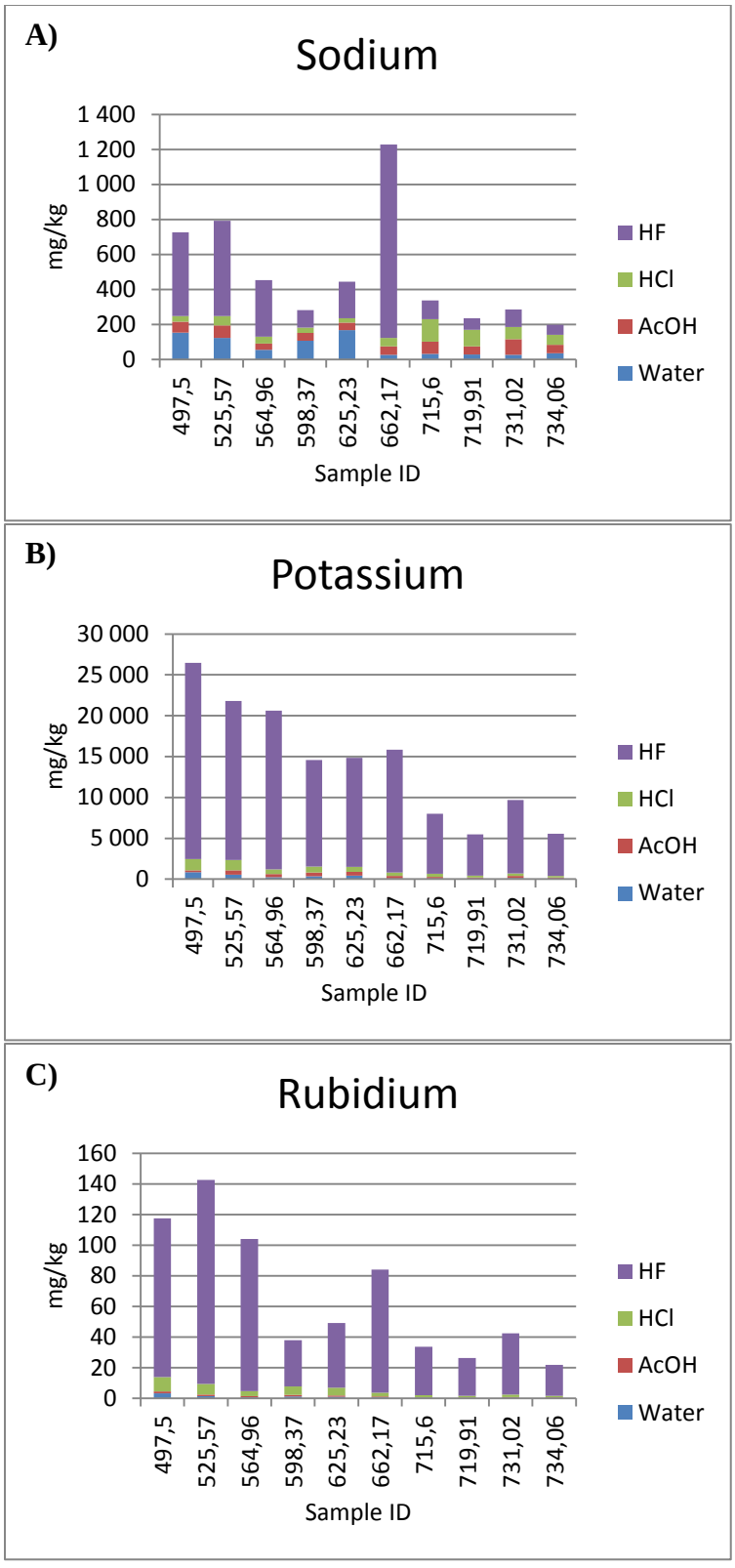

Figure 4.1: Concentrations of monovalent cations in leachates A) Sodium B) Potassium C) Rubidium.

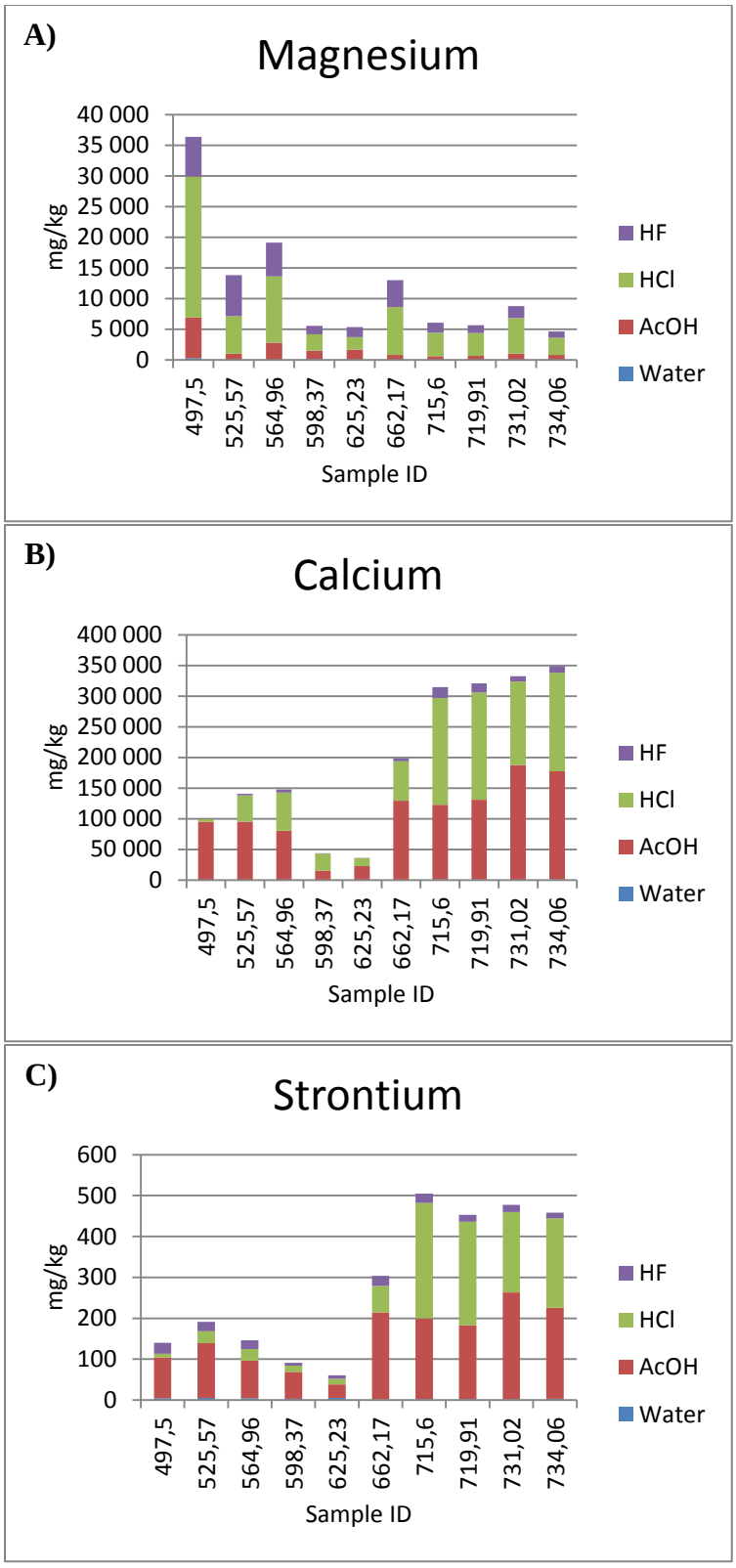

Figure 4.2: Concentrations of divalent cations in leachates A) Magnesium B) Calcium C) Strontium.

4.1.2 Porewaters

Concentrations of cations in porewaters are shown in Table 4.2. They are corrected for both dilution and extraction factors (ref. Table 2.2), and are normalized for one liter of porewater.

Table 4.2: Cations in porewaters

Sample	Depth DGR-1/2 (mBGS)	Mg^{2+} (ppm)	Ca^{2+} (ppm)	Sr^{2+} (ppm)	K^{+} (ppm)	Na^{+} (ppm)	Rb^{+} (ppm)
DGR5-497.50	458.01	10 688	52 215	1 103	12 607	47 869	16.9
DGR5-514.22	473.82	11 102	51 270	1 038	14 133	49 005	18.8
DGR5-525.57	484.59	11 309	54 867	1 214	14 798	51 470	19.3
DGR5-557.65	515.12	5 930	52 567	1 032	13 012	48 547	17.0
DGR5-564.96	522.20	12 415	61 502	1 528	15 198	66 450	20.5
DGR5-598.37	554.92	7 321	35 854	1 002	13 525	46 474	21.5
DGR5-625.23	581.28	7 286	38 973	1 119	12 360	46 817	17.3
DGR6-654.12	582.42	9 520	53 824	1 546	15 190	57 794	18.9
DGR6-661.83	589.11	8 476	52 477	1 474	13 537	59 674	16.9
DGR6-662.17	589.41	11 709	62 213	1 707	13 336	94 772	17.2
DGR6-662.82	589.98	8 228	50 253	1 409	13 452	53 540	16.4
DGR5-649.57	605.17	5 809	46 241	1 246	11 379	53 397	14.0
DGR6-683.25	607.67	6 822	48 430	1 285	12 244	50 791	15.4
DGR6-697.79	619.36	8 787	54 676	1 712	14 338	73 875	17.8
DGR5-671.30	625.33	6 525	44 277	1 220	10 136	51 541	12.2
DGR5-683.57	636.57	9 898	63 336	1 712	14 183	73 912	16.4
DGR5-697.85	649.71	8 988	52 699	1 491	13 042	65 015	14.5
DGR5-715.60	666.57	10 018	39 977	1 707	11 053	59 447	5.05
DGR5-724.60	676.15	10 262	41 153	1 759	10 750	59 900	4.64
DGR5-731.02	682.45	5 924	25 850	977	6 146	34 368	4.70
DGR5-734.06	685.58	11 179	37 893	1 543	12 698	62 004	8.85

Cations in porewaters are, as expected, consistent with analysis done in 2011 (Clark, Scharf, Zuliani, & Herod, 2011). Moreover, they seem to be fairly consistent through depths, except for rubidium, which is found in smaller amounts in the limestone's porewaters. In general, cations in porewaters do not reflect the same trend as

cations in rocks, indicating they are not in equilibrium, nor they are leaching from the rock (Figure 4.3 and Figure 4.4). The only observable exception is potassium concentrations in the HF/HNO_3 solution, which appears to be similar to those of the porewaters. In the Ordovician shales, the dominant clay mineral is illite, which hosts the largest reservoir of potassium. These minerals likely formed by illitization of diagenetic smectite with the infiltration of K-enriched brines during the Silurian, fixing large amounts of potassium and rubidium into the illite interlayers. Moreover, swelling clay minerals (mainly smectite) are found in the shales. Those minerals have the potential to hold large amounts of exchangeable interlayer cations, especially potassium. Being abundant and mobile, those potassium ions can easily reach equilibrium between interlayers and porewaters. If that were to be true, the same trend would be observed in other cations, especially rubidium, which acts like potassium in clays. However, rubidium is more strongly adsorbed onto clays than potassium, therefore has a reduced mobility and has a higher affinity with clay surfaces than with water. This effect probably had an impact when porewaters were originally extracted in 2008, using the crush-and-leach method. This, combined with illitization, could be an explanation for the reduced concentration of Rb in porewaters compared to that of the HF/HNO_3 solution.

Figure 4.3 and Figure 4.4 show the concentration of the different cations through depth for the porewaters and for each leachate of the rock dissolution sequence. Included on those graphs are the concentrations of cations in the Guelph and Cambrian groundwaters (orange dots) (Heagle & Pinder, 2009), (Jackson & Heagle, 2010). Results are plotted by depth relative to DGR-1/2, and not by depth according to the samples labels (ref. Table 3.1 and Figure 3.1). It appears that porewaters have cation

concentrations similar to those of the groundwaters, indicating a possible mixing of the two sources. The only exception is rubidium, which is found in greater concentrations in porewaters than in groundwaters, by a factor of approximately 10, for reasons previously mentioned. Also, strontium in porewaters show a slight enrichment in concentration compared to those of groundwaters. This could at first be explained by the ingrowth through time from the ^{87}Rb decay, but this hypothesis will be analyzed later in the isotopes section. It is already known and that the Silurian marine water (forming today's Guelph groundwater) has infiltrated deeper strata, so such observations are not surprising. Combined with the diffusion of the Cambrian groundwater, both sources can form a mixing line and be an explanation for the origins of porewaters.

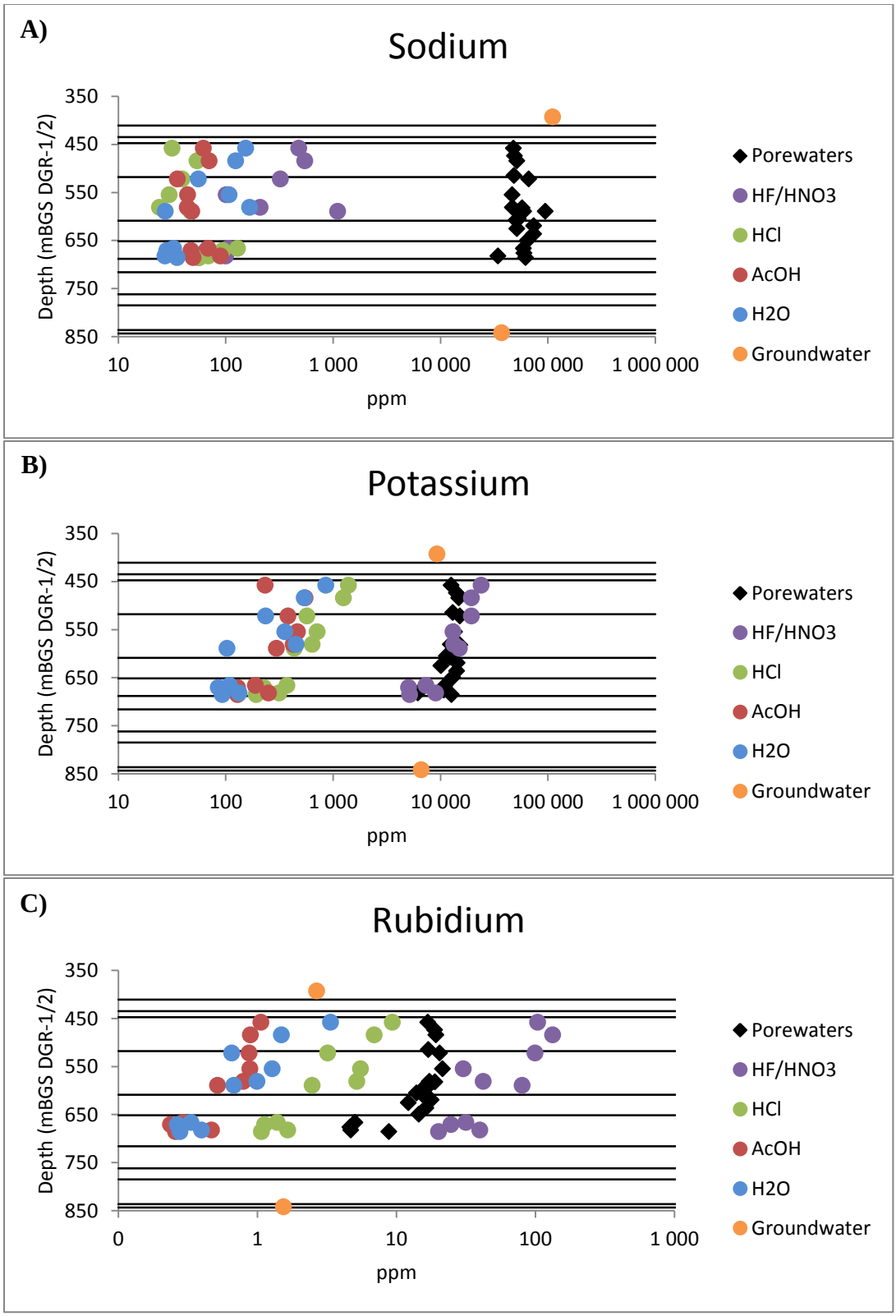

Figure 4.3: Cations in porewaters and leachates. A) Sodium, B) Potassium, C) Rubidium.

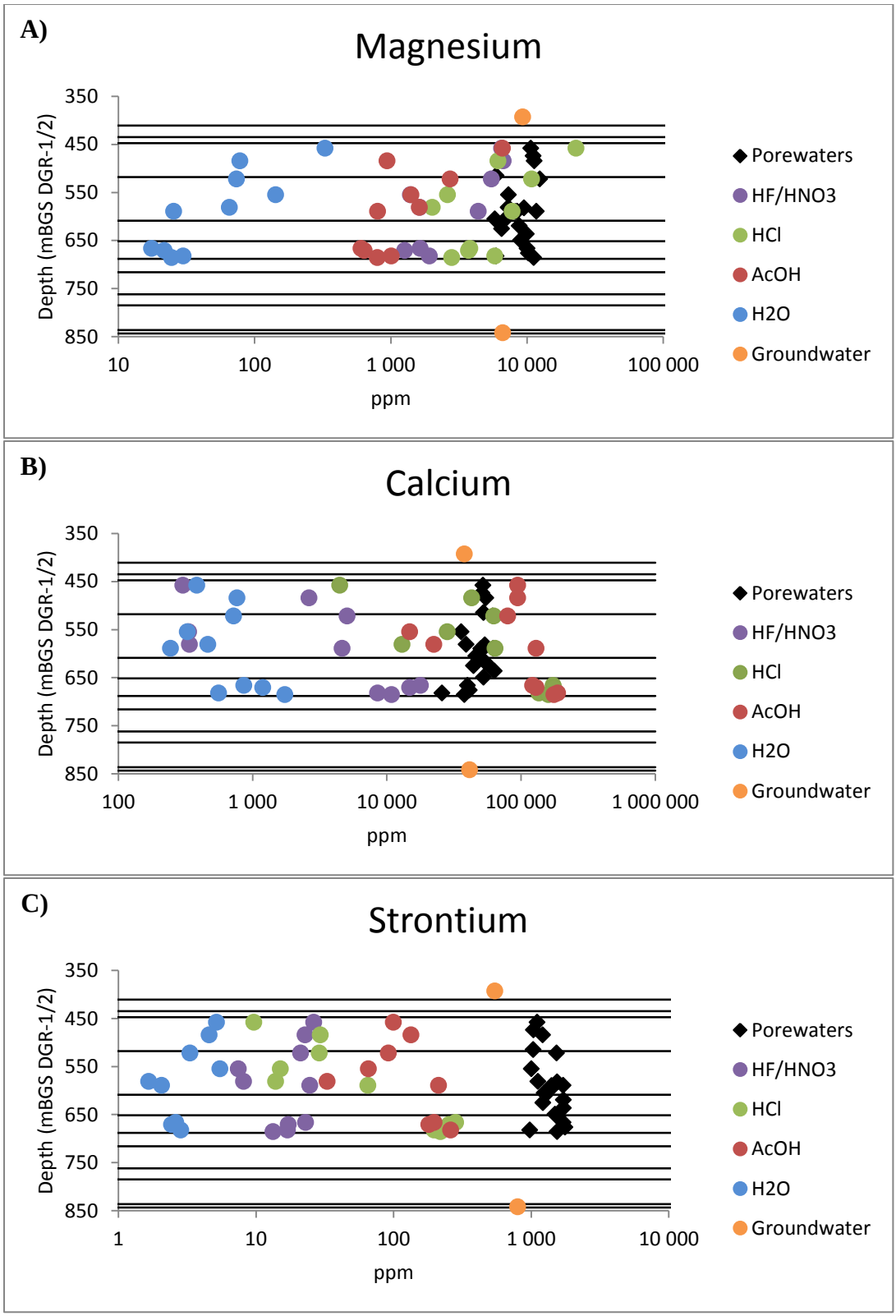

Figure 4.4: Cations in porewaters and leachates A) Magnesium, B) Calcium, C) Strontium.

4.2 Rubidium isotopes

4.2.1 Rocks

As previously mentioned, ^{85}Rb was measured and converted into total rubidium (ref. Table 4.1) and ^{87}Rb with natural abundance ratios. Since ^{87}Rb is the isotope of interest, its concentration is shown in Table 4.3 for each leachate of the rock, expressed in mg/kg of rock (ppm). Note that concentrations for whole rocks were calculated by summing concentrations for each leachate. Concentrations are visually represented in Figure 4.5

Table 4.3: ^{87}Rb in the different leachates of rock samples

Sample	Depth DGR-1/2 (mBGS)	H_2O (ppm)	AcOH (ppm)	HCl (ppm)	HF/HNO_3 (ppm)	Whole rock (ppm)
DGR5-497.50	458.01	0.93	0.30	2.61	28.88	32.71
DGR5-525.57	484.59	0.42	0.25	1.93	37.12	39.70
DGR5-564.96	522.20	0.18	0.24	0.89	27.66	28.97
DGR5-598.37	554.92	0.36	0.25	1.54	8.45	10.58
DGR5-625.23	581.28	0.28	0.22	1.45	11.73	13.67
DGR6-662.17	589.41	0.19	0.14	0.69	22.35	23.37
DGR5-715.60	666.57	0.09	0.08	0.39	8.83	9.39
DGR5-719.91	671.01	0.07	0.07	0.31	6.87	7.33
DGR5-731.02	682.45	0.11	0.13	0.46	11.09	11.79
DGR5-734.06	685.58	0.08	0.07	0.30	5.60	6.05

Since concentrations of ^{87}Rb are directly derived from ^{85}Rb measurements, they follow the same trends. Those values will be used for calculations later in section 4.4.

4.2.2 Porewaters

Just like for rocks, ^{87}Rb in porewaters were derived from ^{85}Rb measurements and follow the same trend as presented in Table 4.2. Concentrations of rubidium-87 are presented in Table 4.4, expressed in ppm.

Table 4.4: ^{87}Rb in porewaters

Sample	Depth DGR-1/2 (mBGS)	^{87}Rb (ppm)
DGR5-497.50	458.01	4.70
DGR5-514.22	473.82	5.24
DGR5-525.57	484.59	5.37
DGR5-557.65	515.12	4.73
DGR5-564.96	522.20	5.71
DGR5-598.37	554.92	5.97
DGR5-625.23	581.28	4.82
DGR6-654.12	582.42	5.27
DGR6-661.83	589.11	4.70
DGR6-662.17	589.41	4.78
DGR6-662.82	589.98	4.55
DGR5-649.57	605.17	3.89
DGR6-683.25	607.67	4.29
DGR6-697.79	619.36	4.96
DGR5-671.30	625.33	3.40
DGR5-683.57	636.57	4.56
DGR5-697.85	649.71	4.04
DGR5-715.60	666.57	1.41
DGR5-724.60	676.15	1.29
DGR5-731.02	682.45	1.31
DGR5-734.06	685.58	2.46

Figure 4.5 shows ^{87}Rb profiles for all leachates and porewaters, all reported in ppm. Trends are very similar to those observed in Figure 4.3c, as ^{87}Rb concentrations are directly proportional to total rubidium.

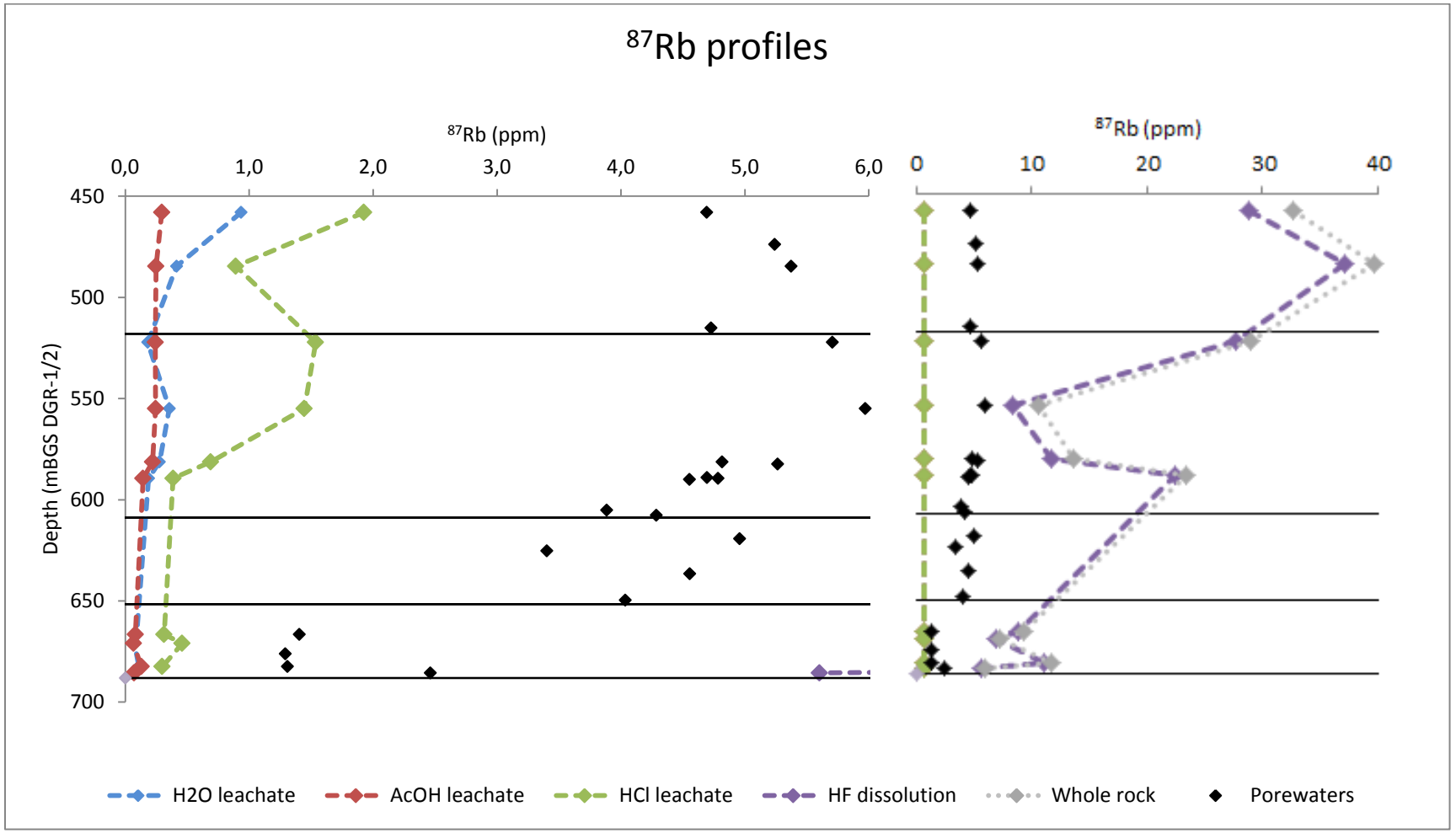

Figure 4.5: ^{87}Rubidium in leachates and in porewaters

4.3 Strontium isotopes

4.3.1 Rocks

Measured values of strontium isotopes ratios are presented in Table 4.5. Since strontium isotopes are expressed in absolute ratios, they are dimensionless. Whole rock isotopic signatures were calculated using the following equation:

$$\left(\frac{^{87}Sr}{^{86}Sr}\right)_{Whole\ Rock} = \frac{\sum\left(\left(\frac{^{87}Sr}{^{86}Sr}\right)_{leachate} * [Sr]_{leachate\ (\frac{mmol}{kg})}\right)}{\sum[Sr]_{leachate\ (\frac{mmol}{kg})}} \qquad \text{Equation 4.1}$$

where $(^{87}Sr/^{86}Sr)_{leachate}$ *and* $[Sr]_{leachate\ (mmol/kg)}$ represent respectively the strontium isotopes ratios and the concentration of strontium, expressed in mmol/kg, for each leachate. 2σ was calculated for whole rocks, deriving the previous equation.

Table 4.5: Strontium isotopes ratios in rocks

Sample	Depth DGR-1/2 (mBGS)	H_2O		AcOH		HCl		HF		Whole rock	
		$^{87}Sr/^{86}Sr$	$\pm 2\sigma$	$^{87}Sr/^{86}Sr$	$\pm 2\sigma$	$^{87}Sr/^{86}Sr$	$\pm 2\sigma$	$^{87}Sr/^{86}Sr$	$\pm 2\sigma$	$^{87}Sr/^{86}Sr$	$\pm 2\sigma$
DGR5-497.50	458.01	0.72299	0.00004	0.70919	0.00001	0.7263	0.0001	0.79236	0.00001	0.7264	0.0413
DGR5-525.57	484.59	0.71368	0.00002	0.70886	0.00003	0.71150	0.00002	0.79360	0.00001	0.7195	0.0317
DGR5-564.96	522.20	0.71186	0.00002	0.70904	0.00006	0.70975	0.00002	0.78228	0.00007	0.7199	0.0357
DGR5-598.37	554.92	0.72338	0.00002	0.71029	0.00002	0.71410	0.00002	0.78879	0.00001	0.7178	0.0564
DGR5-625.23	581.28	0.71223	0.00001	0.71053	0.00002	0.71358	0.00001	0.78066	0.00002	0.7208	0.0643
DGR6-662.17	589.41	0.71155	0.00002	0.70846	0.00006	0.70917	0.00002	0.76230	0.00002	0.7130	0.0200
DGR5-715.60	666.57	0.70966	0.00003	0.70817	0.00001	0.70805	0.00001	0.73280	0.00002	0.7092	0.0103
DGR5-719.91	671.01	0.70949	0.00002	0.70817	0.00002	0.70801	0.00002	0.73424	0.00002	0.7091	0.0114
DGR5-731.02	682.45	0.71054	0.00004	0.70813	0.00002	0.70812	0.00002	0.75409	0.00002	0.7098	0.0108
DGR5-734.06	685.58	0.70944	0.00002	0.70818	0.00002	0.70804	0.00002	0.74092	0.00002	0.7090	0.0111

It is already known that limestones were precipitated from the seawater. Thus, it is expected that the strontium isotope signatures of the carbonates (from the acetic acid and hydrochloric acid leachates) to be the same than that of the seawater at the time of deposition. As for the shales (DGR5-497.50 to DGR6-662.17) containing less carbonates, they were not formed the same way than the Ordovician limestones, thus it would be surprising that the associated AcOH and HCl leachates show the seawater values (Spencer, 2013). The HF/HNO_3 solutions, on the other hand, were expected to have very high ratios, as they are rich in clays, thus concentrated in rubidium and have a high potential for ^{87}Sr enrichment. Measured values for strontium isotopes ratios are consistent with what was expected, based on rubidium contents. More explanations on the values will be found in the next section, along with porewater values.

4.3.2 Porewaters

Strontium isotope ratios in porewaters are presented in Table 4.6. The first observation is that ratios in porewaters show relatively constant values, slightly increasing with depth, which is consistent with the initial observation made in 2011 (ref. Figure 1.1).

Table 4.6: Strontium isotopes in porewaters

Sample	Depth DGR-1/2 (mBGS)	$^{87}Sr/^{86}Sr$	± 2σ
DGR5-497.50	458.01	0.70965	0.00005
DGR5-514.22	473.82	0.70964	0.00003
DGR5-525.57	484.59	0.70970	0.00002
DGR5-557.65	515.12	0.70971	0.00003
DGR5-564.96	522.20	0.70983	0.00002
DGR5-598.37	554.92	0.70988	0.00002
DGR5-625.23	581.28	0.70990	0.00002
DGR6-654.12	582.42	0.70992	0.00002
DGR6-661.83	589.11	0.70991	0.00002
DGR6-662.17	589.41	0.70987	0.00003
DGR6-662.82	589.98	0.70991	0.00003
DGR5-649.57	605.17	0.70993	0.00002
DGR6-683.25	607.67	0.70992	0.00003
DGR6-697.97	619.36	0.70989	0.00002
DGR5-671.30	625.33	0.70992	0.00002
DGR5-683.57	636.57	0.70994	0.00003
DGR5-697.85	649.71	0.70993	0.00003
DGR5-715.60	666.57	0.70988	0.00001
DGR5-724.60	676.15	0.70996	0.00002
DGR5-731.02	682.45	0.70989	0.00002
DGR5-734.06	685.58	0.70997	0.00003

Strontium isotope ratios of porewaters and of each leachate of rocks and are plotted in Figure 4.6 along with ratios of seawater from the Ordovician and Silurian (Veizer J. , 1989). Results will be discussed in the following section.

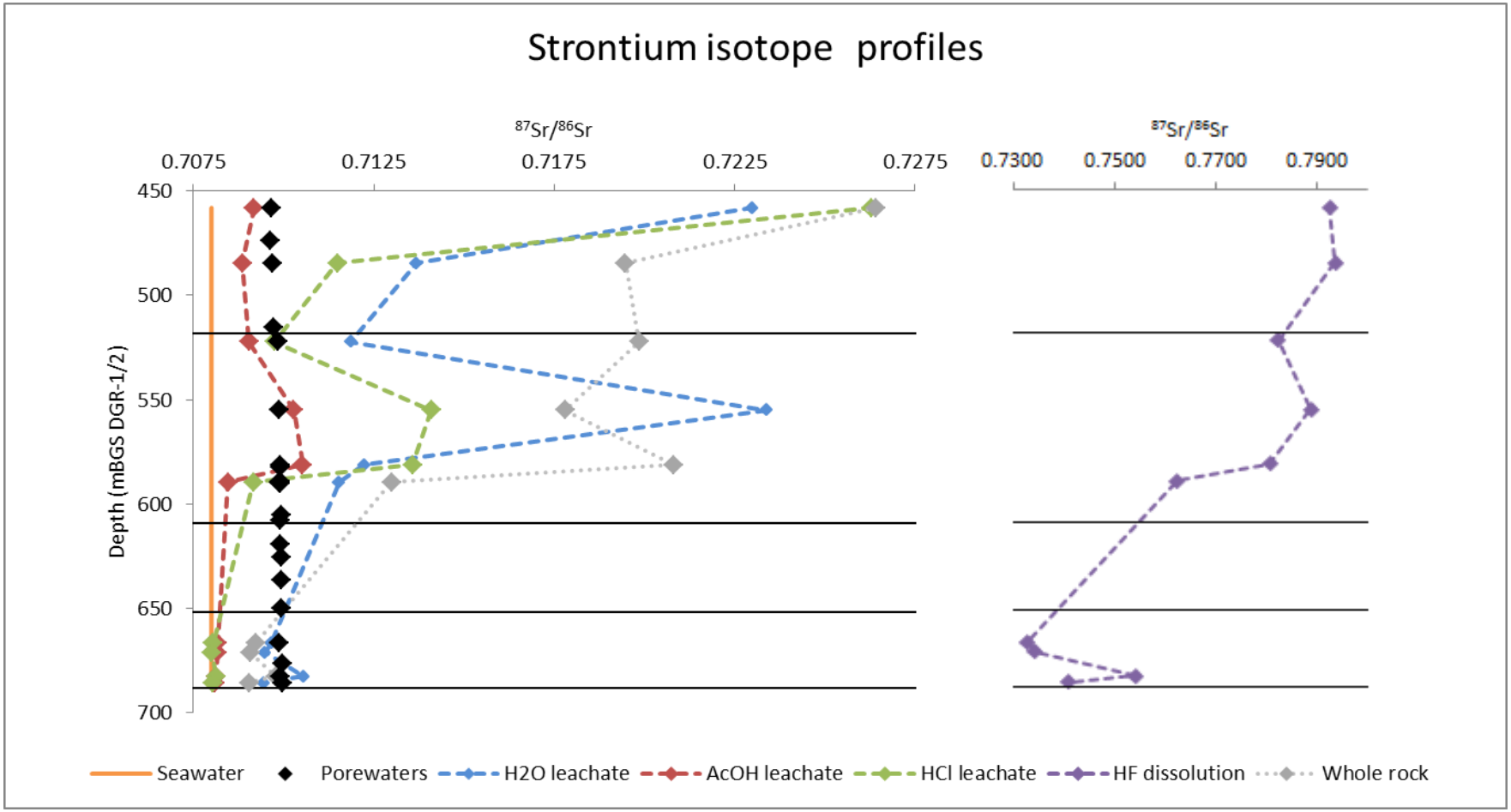

Figure 4.6: Strontium isotope profiles in porewaters and in rocks. Seawater value from Veizer (1999).

4.4 Dynamics

4.4.1 Equilibrium between rocks and porewaters

The first observation from Figure 4.6 is that strontium signatures of porewaters are in total discordance with any phase of the rock, suggesting leaching of rocks by pore fluids is very unlikely. In that case, strontium signatures in porewaters would have reflected that of the rock, or at least one of the phases, since they would have reached equilibrium over time. Moreover, concentrations of radiogenic strontium should be directly derived from concentrations of radioactive rubidium. Thus, if clays were to exclude radiogenic strontium in porewaters when it is formed, the isotopic ratio of strontium in porewaters would reflect the trends of rubidium in clays. Figure 4.5 and Figure 4.6, show that it is not the case, thus this hypothesis has to be rejected.

Another interesting observation can be made when comparing Figure 4.5 and Figure 4.6. In the three first leachates, strontium isotopes ratios follow approximately the same trend as rubidium-87 concentrations. The HF/HNO_3 curve for ^{87}Rb shows a negative excursion at the Queenston depths (518-609 m) while strontium isotopes are going the other way. That could be intriguing at first sight, but a few calculations are enough to prove it is still consistent. Using isotopes and concentrations of both elements, it is possible to calculate the potential strontium isotopes ratio of a sample after a given amount of time. Exhaustive calculations are shown in Appendix B. When applying these calculations to each phase of the rock, using 0.7080 as initial ratio, the potential final $^{87}Sr/^{86}Sr$ ratio is calculated. It is then possible to compare it to measurements in each leachate. Calculations were performed using 450 million years (estimated time elapsed since deposition) for H_2O, AcOH and HCl leachates, and 415 million years for the HF

solution, since illites likely formed after the infiltration of the Silurian brine. Figure 4.7 shows profiles for measured ratios (dashed lines) along with calculated final ratios (solid lines).

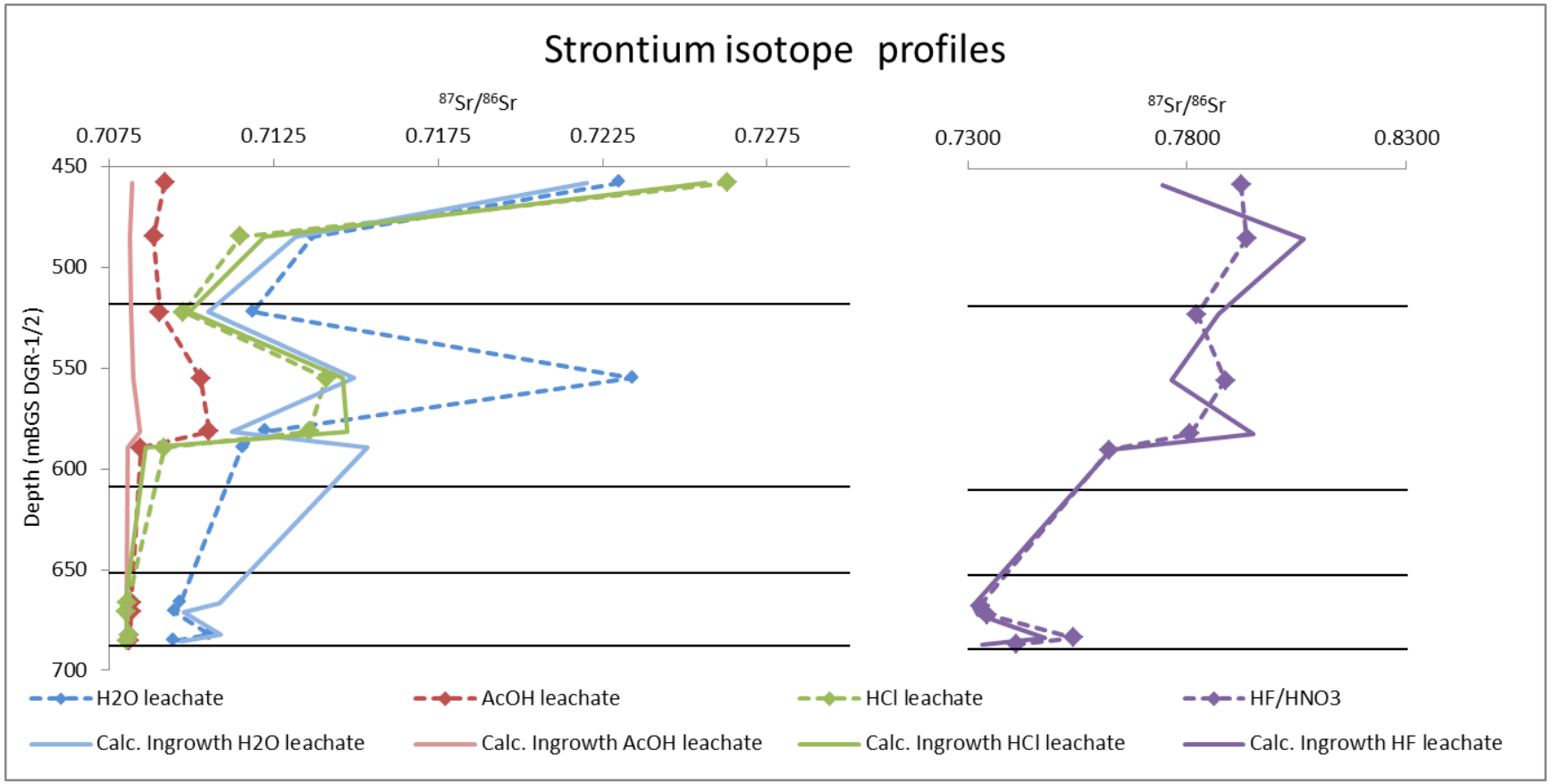

Figure 4.7: Measured $^{87}Sr/^{86}Sr$ and calculated ingrowth from ^{87}Rb in each phase of the rock

Although ^{87}Rb in for the HF curve was not consistent with measured strontium isotopes in Figure 4.5, when considering the original amount of ^{87}Sr in samples, it is still possible to get approximately to the measured values.

Hydrochloric acid leachates have strontium isotopes signatures very similar to what would be expected with calculated ingrowths, suggesting this phase has not been exchanging any rubidium or strontium since it has been formed. On the other hand, acetic acid leachates seem to contain too little rubidium to decay to the measured strontium isotopes values. When Silurian brines have infiltrated the Ordovician depths, they caused dolomitization that changed strontium isotopic ratios, since the brine was richer in radiogenic strontium (up to 0.7088 during the Silurian) (ref. Figure 2.6).

$$2CaCO_{3\ calcite} + Mg^{2+} \leftrightarrow CaMg(CO_3)_{2\ dolomite} + Ca^{2+}$$

$$CaCO_{3\ calcite} + Sr^{2+} \leftrightarrow SrCO_{3\ strontianite} + Ca^{2+}$$

Strontium in those brines had an enriched value of $^{87}Sr/^{86}Sr$ compared to calcite, resulting in the formation (to trace levels) of enriched strontianite. When leaching those rocks with acetic acid, strontianite dissolved (Bolton, 1878), causing the measured value of $^{87}Sr/^{86}Sr$ to be higher than expected.

4.4.2 Ingrowth from groundwater

It is proven that the ingrowth of ^{87}Sr in porewaters cannot be attributed to leaching of rocks or ^{87}Sr exclusion. That leaves only one other possibility: ingrowth of ^{87}Sr in the caused by the ^{87}Rb decay in the porewaters themselves. In that case, the original strontium isotopes ratios of porewaters have to be determined. Geochemical analysis showed porewaters likely originated from a mixture of both Guelph and Cambrian groundwater, but another option is

that they find their origin in seawater trapped in pores when rocks formed. Both possibilities have to be considered.

When taking concentrations of both rubidium and strontium, combined with isotopes of both elements in porewaters, it is possible to calculate the original $^{87}Sr/^{86}Sr$ in porewaters 415 000 000 years ago (estimated age of the Silurian brine). However, this calculation will be valid only in the case where no external sources of rubidium or strontium mixed with the porewater, and where none of the elements precipitated or were lost by any process. Exhaustive calculations are found in Appendix C.

Figure 4.8 represents measured strontium isotopes ratios for porewaters (black diamonds), as well as those from both Guelph and Cambrian groundwaters (light blue dashed line) (Heagle & Pinder, 2009). Guelph groundwater has undergone ^{87}Rb decay over time as well; its value is represented (dark blue dot). For the Cambrian groundwater, Raven et al. (2011) raised the possibility that radiogenic $^{87}Sr/^{86}Sr$ observed in the Middle Ordovician limestones porewaters comes from the underlying Precambrian rocks. Enriched brines from the Precambrian were measured in Sudbury (McNutt, Frape, & Fritz, 1984). Movement of strontium into the overlying rocks, probably mixing with the Guelph groundwater, is consistent with observations of other parameters such as δD and $\delta^{18}O$ (Raven, et al., 2011). As a result, the original value for the Cambrian groundwater was set to 0.71035, which represents the average between the Precambrian brines and the original Cambrian groundwater values. The resulting mixing line between the original Guelph and Cambrian groundwaters is plotted (dark blue line). The graph also shows back-calculated original ratios of porewaters (green stars) as well as the calculated ingrowth of radiogenic strontium by ^{87}Rb decay in porewaters (red diamonds).

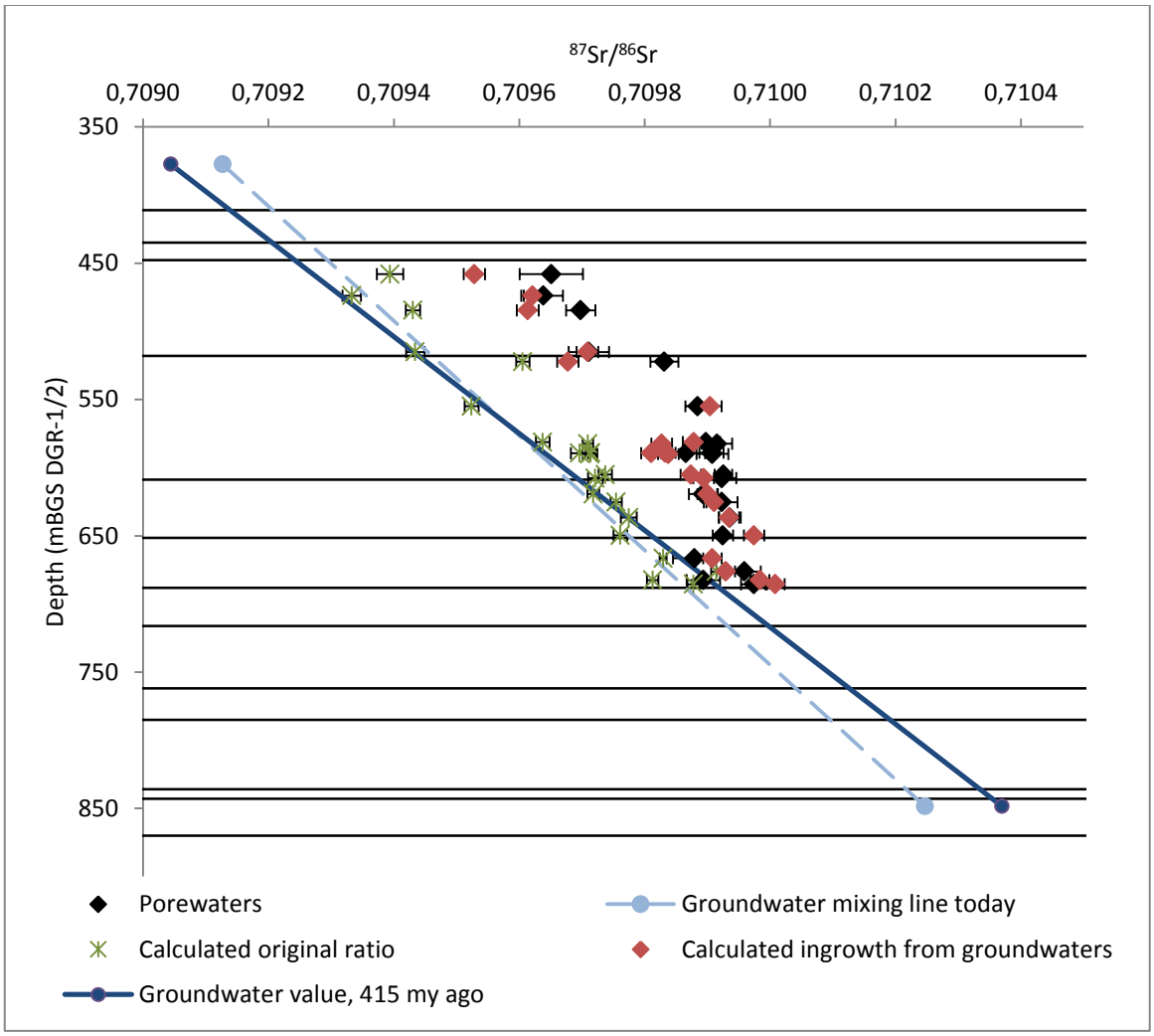

Figure 4.8: Original $^{87}Sr/^{86}Sr$ of porewaters and calculated ingrowth

The calculated original ratios show a strong correlation with the groundwaters mixing line. This observation adds to the proof that porewaters originate from the infiltrated Guelph groundwater and the diffusion of the Cambrian groundwater, likely mixed with Precambrian brines. The calculated values for the ingrowth of ^{87}Sr in porewaters (Appendix C) are also consistent with measurements, with very little variation. These calculations were performed with the original groundwater values (dark blue line).

4.4.3 Ingrowth from seawater

Constant strontium isotopes ratios in porewaters could lead thinking that they originate from seawater trapped in pores when rocks were formed, and that ^{87}Sr has been ingrowing overtime. The main difference between this scenario and the previous one is the original strontium isotopes ratio of the water. In section 4.4.2, the original value was the mix of both groundwaters. Here, it is the seawater ratio, 0.7080 (ref. Figure 2.6). Calculations from the previous section were performed again considering this different parameter. Results are plotted in Figure 4.9 (black line).

Furthermore, ^{87}Rb content in rocks was used to calculate the potential ingrowth of strontium in the case that ^{87}Sr were to be expelled in porewaters once formed in minerals. Although it is already demonstrated that this process does not take place in the system, this consideration now adds to the proof that leaching from the rocks does not occur. For each sample of porewater, the original amount of ^{87}Sr was added to the ^{87}Sr formed by ^{87}Rb decay in porewaters and to the entire amount of ^{87}Sr formed by ^{87}Rb decay in each phase of the matching rock sample. Full calculations are shown in Appendix D, and results are shown in Figure 4.9. Calculations were performed for each phase of the rock, as well as for the whole rock, considering 450 000 000 years (estimated time elapsed since deposition).

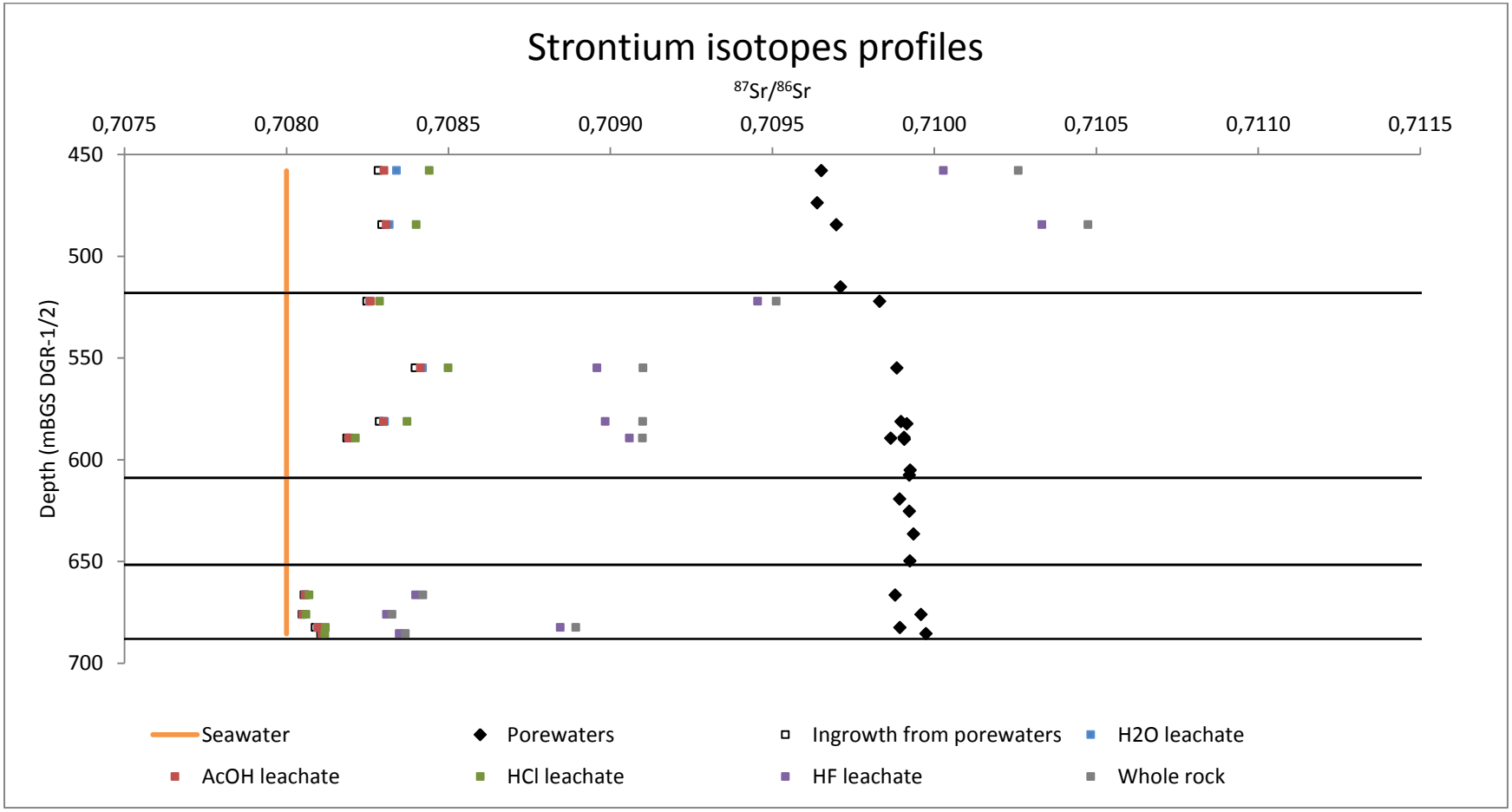

Figure 4.9: Calculated strontium isotopes ratios in porewaters, considering 450 000 000 years for ^{87}Rb decay

Figure 4.9 shows it would be impossible to reach the $^{87}Sr/^{86}Sr$ in porewaters when considering their original ratio is that of the seawater (0.7080)., even when releasing 100% of the decayed rubidium (in 450 m.y.) from the rock into the porewaters. With the exception of the two uppermost Queenston samples, the value is still far from the measured ratio in most samples. Thus, the hypothesis suggesting the porewaters originate from infiltrated and diffused groundwater remains the most plausible.

4.4.4 Strontium and Rubidium isotopes as a dating tool

One of the major problems when using the Rb-Sr method to date rocks is that calculated ages are those of the formation of the rock, which is not necessarily the same as its deposition. For sedimentary rocks, this rests on the assumption that all phases of the rock were formed at the same time and were not transported, that strontium isotopes were homogenized within the rock during its formation, and that the system remained close until today. In the case of the studied Ordovician shales and limestones, isochrons were traced and interpreted to have a better understanding of the interactions.

Isochrons were plotted for each leachate (Figure 4.10), with measured strontium isotopes ratios and with calculated ingrown ^{87}Sr from ^{87}Rb. A time of 450 million years was used in calculations for H_2O, AcOH and HCl leachates, and 415 million years was used for HF/HNO_3 dissolution, as illites likely formed with the Silurian brines (see calculations in Appendix B). Table 4.7 shows, for each isochron, the value of the slope, intercept, determination coefficient (r^2) as well as the calculated age obtained from those parameters.

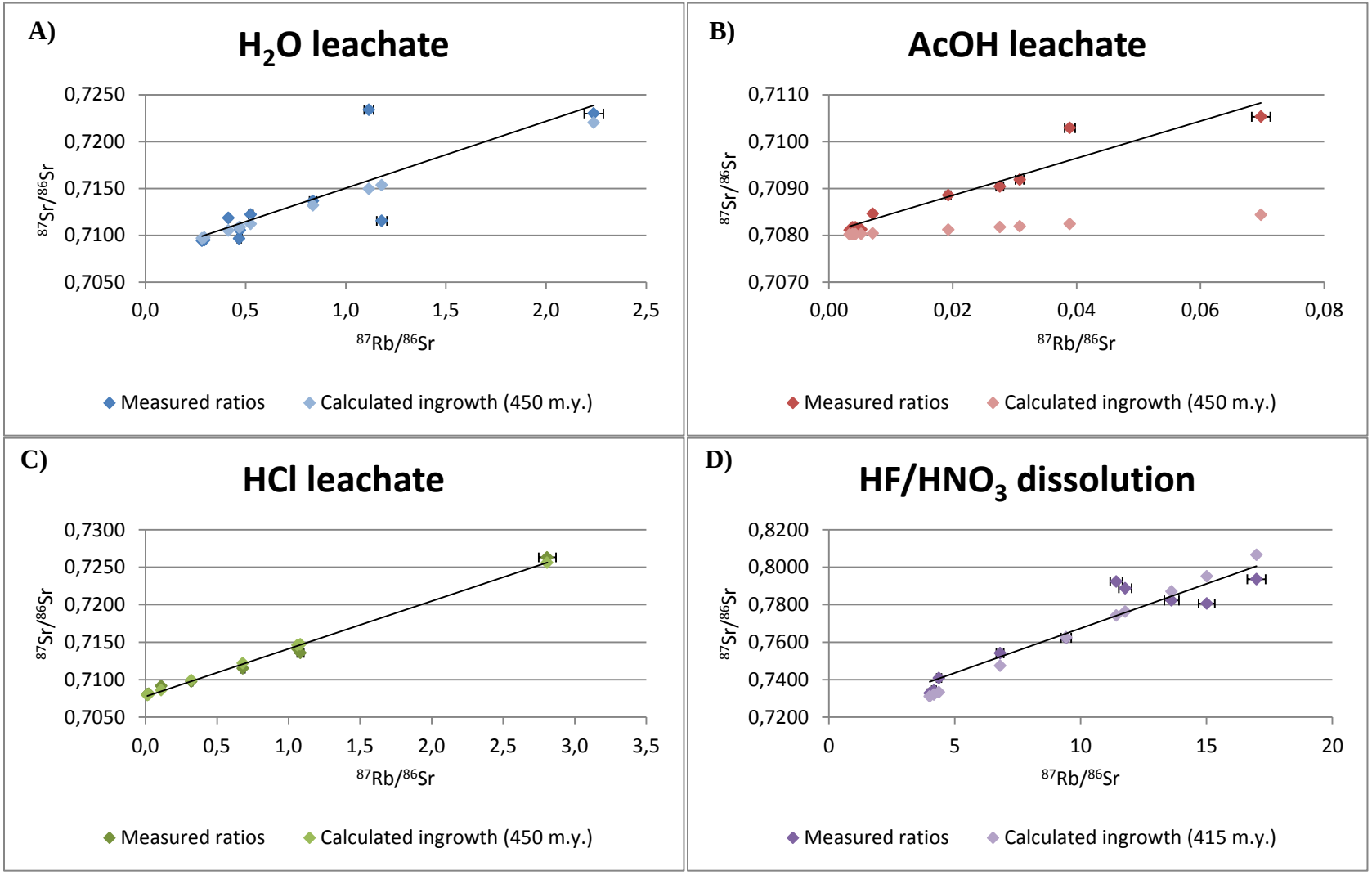

Figure 4.10: Isochrons for A) Water leachate, B) Acetic acid leachate, C) Hydrochloric acid leachate, D) Hydrofluoric acid dissolution.

Table 4.7: Statistical parameters and calculated age for each isochron

Leach	Slope	Intercept	r^2	Calculated age (years)	
H_2O	0.0071	0.7079	0.6625	509 300 000	± 128 000 000
AcOH	0.0369	0.7081	0.9123	2 779 300 000	± 298 900 000
HCl	0.0064	0.7078	0.9902	453 700 000	± 15 900 000
HF/HNO_3	0.0048	0.7198	0.8613	339 700 000	± 48 000 000

In the first three isochron, values of intercepts reflect that of the seawater (0.7080), with minor differences. That is consistent with the fact that rocks dissolved in those three leachates are mostly evaporites and carbonates, deposited from marine environments. Values for the water leachate isochron do not show a very strong correlation (r^2=0.6625), mostly because this leachate did not target any mineral specifically. Celestite have probably dissolved at this step (Reardon & Armstrong, 1987), with a few other evaporites and adsorbed ions. As a result, a trend is observable, the calculated age is consistent, but the correlation is weak.

The acetic acid isochon is also consistent with Figure 4.7 where it was shown that calcite does not contain enough rubidium to get to the measured strontium isotopes ratios. However, the isochron shows a strong correlation between the ratios and $^{87}Rb/^{86}Sr$, suggesting not only calcite was dissolved by acetic acid. Strontianite, formed along with dolomite (see section 4.4.1) has probably dissolved at this step, enriching the $^{87}Sr/^{86}Sr$ in leachates. As a result, the calculated age is not representative of reality. On the other hand, the hydrochloric acid isochron, which represents dolomite, is exactly as expected. Its calculated age of 453 700 000 years and its strong correlation (r^2 = 0.9902) are consistent with the estimated time of deposition for carbonates.

Finally, the HF/HNO_3 isochron shows a significant correlation between the two isotopes ratios. The calculated age of 339.7 million years corresponds to the age of illitization, when the original smectites were converted to illite by uptake of K and Rb from the infiltrating Silurian brine.

It is impossible to trace such isochrons for porewaters, since each sample has a different $^{87}Sr/^{86}Sr$ original value from the mixing line. However, ages can be calculated for each sample individually. Stable isotopes (D, ^{18}O, ^{3}He, $^{13}CH_4$, and $^{13}CO_2$) provided evidence for porewater residence time approaching the age of the rock (Al, Clark, Kennell, Jensen, & Raven, 2014) (Clark, et al., 2013) (Clark, et al., 2013). They were also used to prove the system remained close since the Silurian brine infiltration. All conditions being met to date pore fluids, estimations of their age were obtained by calculating the difference between the estimated original mixing line and the measured values (ref. Figure 4.8). For each sample, the calculated age is reported in Table 4.8.

Table 4.8: Estimated ages of porewaters

Sample	Depth (mBGS DGR-1/2)	Calculated age (years)	
DGR5-497.50	458.01	621 600 000	± 58 500 000
DGR5-514.22	473.82	445 900 000	± 34 300 000
DGR5-525.57	484.59	553 800 000	± 34 100 000
DGR5-557.65	515.12	425 700 000	± 37 100 000
DGR5-564.96	522.20	705 400 000	± 40 500 000
DGR5-598.37	554.92	397 000 000	± 22 700 000
DGR5-625.23	581.28	452 100 000	± 31 900 000
DGR6-654.12	582.42	599 900 000	± 35 500 000
DGR6-661.83	589.11	581 900 000	± 35 500 000
DGR6-662.17	589.41	559 500 000	± 59 600 000
DGR6-662.82	589.98	571 400 000	± 45 500 000
DGR5-649.57	605.17	536 900 000	± 43 700 000
DGR6-683.25	607.67	481 700 000	± 42 800 000
DGR6-697.97	619.36	406 000 000	± 38 600 000
DGR5-671.30	625.33	454 000 000	± 39 400 000
DGR5-683.57	636.57	425 700 000	± 54 300 000
DGR5-697.85	649.71	297 200 000	± 44 300 000
DGR5-715.60	666.57	200 200 000	± 79 600 000
DGR5-724.60	676.15	713 400 000	± 144 600 000
DGR5-731.02	682.45	(34 000 000)[1]	± 67 800 000
DGR5-734.06	685.58	280 200 000	± 68 700 000

[1]*Measured $^{87}Sr/^{86}Sr$ is smaller than the original estimated value by the mixing line. See Figure 4.8.*

Samples from the shales (DGR5-497.50 to DGR5-697.85) show ages fairly consistent with the Ordovician. Variations and large uncertainties are attributed to the approximation of the original $^{87}Sr/^{86}Sr$ values by the mixing line between both groundwaters (ref. Figure 4.8), and to the fact that rubidium is exchanging with clays at an unknown rate. As for limestones (DGR5-715.60 to DGR5-734.06), their estimated age is much lower than reality. This could be attributed to their very low concentration in rubidium, but also to the difficulty setting a value of $^{87}Sr/^{86}Sr$ in the Cambrian groundwater, as the exchange rate between this water and the Precambrian brines is undetermined.

5.0 CONCLUSIONS

This study shows that the use of geochemistry, combined with rubidium and strontium isotopes, can help understanding the dynamics between rocks and pore fluids. These methods were used to complete the three primary objectives of this thesis, which were (1) to determine the origin of porewaters, (2) to explain the difference in strontium isotopes ratios between the host rocks and their porewaters, and (3) to estimate ages of both rocks and porewaters in the Ordovician shales and limestones, at the DGR site, in Kincardine, Ontario.

5.1 Origin of porewaters

When calculating the original $^{87}Sr/^{86}Sr$ ratio from the measured ratios in porewaters, values corresponding to a mixing line between the Guelph and Cambrian groundwaters were obtained. This suggests porewaters are the result of a mix between the overlying Silurian brines that infiltrated the system, and upward diffusion of the Cambrian groundwaters, likely mixed with Precambrian brined to some extent. This explanation is consistent with other observations from this site (Raven, et al., 2011).

The Ordovician seawater has an $^{87}Sr/^{86}Sr$ of 0.7080. Starting with this original amount of ^{87}Sr, it is impossible to reach the measured values of $^{87}Sr/^{86}Sr$ when taking ^{87}Rb decay into account.

5.2 Ingrowth of ^{87}Sr

Isotopes of both elements showed that the ingrowth of radiogenic strontium in porewaters cannot be caused by pore fluids leaching rocks, as their isotope ratios would have equilibrated over time. Also, it is very unlikely that radiogenic strontium, once

formed by ^{87}Rb decay, is expelled from minerals and transferred into porewaters. In that case, ^{87}Rb in rocks and $^{87}Sr/^{86}Sr$ in porewaters would follow the same trends. The ingrowth of ^{87}Sr was thus attributed to the ^{87}Rb decay in porewaters themselves. Calculations support this explanation.

5.3 Rb-Sr dating

Ages were estimated for pore fluids and isochrones were traced for each phase of the rocks using strontium and rubidium isotopes. The hydrochloric acid leachates, mostly containing dolomites, gave a reliable age (453 700 000 years before present) corresponding to that of their deposition. The HF/HNO_3 isochron gave an age that could correspond to that of illitization, as the process took place after rocks were deposited. The estimated age is 339.7 million years.

5.4 Recommendations

Should additional investigations be conducted to evaluate the age of rocks or porewaters, it is recommended that other isotopes systems be used to compare results. Analyses of other isotopes systems could also add to the understanding of the water-rock interaction at this site.

Furthermore, additional investigations on clays are suggested to differentiate ions and isotopes from the interlayers than those from their structures. This could provide clues on their real age of formation and how they interacted with the pore fluids and other phases of rocks.

On a technical level, it is suggested to conduct extensive analyses to determine the best conditions required to dissolve each mineral during the leaching sequence. Different

times of reaction, temperatures, and many more chemicals could be tried to dissolve various minerals. Moreover, analyses of the remaining rocks after each leach should be conducted to determine what minerals were dissolved in each leachate.

REFERENCES

Al, T., Clark, I. D., Kennell, L., Jensen, M., & Raven, K. (2014). Geochemical Evolution and Residence Time of Porewater in Low-Permeability Rocks of the Michigan Basin, Southwest Ontario. *Unpublished*.

Anderson, D. L. (1989). *Theory of the Earth.* Boston: Blackwell Scientific Publications.

Armstrong, D. K., & Carter, T. R. (2010). *The Subsurface Paleozoic Stratigraphy of Southern Ontario.* Ontario Geological Survey, Special Volume 7.

Bailey, T. R., McArthur, J. M., Prince, H., & Thirlwall, M. F. (2000). Dissolution methods for strontium isotope stratigraphy: whole rock analysis. *Chemical Geology, 167*, 313-319.

Bofinger, V. M., Compston, W., & Vernon, M. J. (1968). The application of acid leaching ot the Rb-Sr dating of a Middle Ordovician shale. *Geochimica et Cosmochimica Acta, 32*, 823-833.

Bolton, H. C. (1878). Application of organic acids to the examination of minerals. (W. Crookes, Ed.) *The Chemical News and Journal of Industrial Science, 37*(951), 65-67.

Burke, W. H., Denison, R. E., Hetherington, E. A., Koepnick, R. B., Nelson, H. F., & Otto, J. B. (1982). Variation of seawater 87Sr/86Sr through Phanezoroic time. *Geology, 10*, 516-519.

Capo, R. C., Stewart, B. W., & Chadwick, O. A. (1998). Strontium isotopes as tracers of ecosystem processes: theory and methods. *Geoderma, 82*(1-3), 197-225.

Carleton University. (2012). *Isotope Geochemistry and Geochronology Research Centre*. Retrieved 09 11, 2014, from Isotope Geochemistry and Geochronology Research Centre: http://iggrc.carleton.ca/

Chaudhuri, S., & Brookins, D. G. (1969). The Rb-Sr Whole-Rock Age od the Stearns Shale (Lower Permian), Eastern Kansas, before and after Acid Leaching Experiments. *Geological Society of America Bulletin, 80*, 2605-2610.

Chaudhuri, S., & Clauer, N. (1992). History of Marine Evaporites : Constraints from Radiogenic Isotopes. (N. Clauer , & S. Chaudhuri, Eds.) *Lecture Notes in Earth Sciences, 43*, 177-198.

Clark, I. D., Al, T., Jensen, M., Kennell, L., Mazurek, M., Mohapatra, R., & Raven, K. (2013). Paleozoic-aged brine and authigenic helium preserved in an Ordovician shale aquiclude. *Geological Society of America, 41*(9), 951-954.

Clark, I. D., Ilin, D., Jackson, R., Jensen, M., Kennell, L., Mohammadzadeh, H., . . . Xing, Y. (2013). Microbial methane of Paleozoic age preserved in Ordovician shales od the Michigan basin, Kincardine, Ontario. *Unpublished*.

Clark, I., & Fritz, P. (1997). *Environmental Isotopes in Hydrogeology.* Boca Raton, Florida: CRC Press.

Clark, I., Scharf, V., Zuliani, J., & Herod, M. (2011). *Porewater Analyses in DGR-5 and DGR-6 Core, Technical Report TR-09-07.* DGR Site Characterization Document, Geofirma Engineering, Toronto.

Clauer, N., Chaudhuri, S., Kralik, M., & Bonnot-Courtois, C. (1993). Effects of experimental leaching on Rb-Sr and K-Ar isotopic systems and REE contents of diagenetic illite. *Chemical Geology, 103*, 1-16.

de Laeter, J. R., Böhlke, J. K., De Bièvre, P., Hidaka, H., Peiser, H. S., Rosman, K. J., & Taylor, P. D. (2003). Atomic weights of the elements. Review 2000 (IUPAC Technical Report). *Pure and Applied Chemistry*, *75*(6), 683-800.

Donaldson, W. S. (1989). The depositional environment of the Queenston Shale, southwestern Ontario. *Proceedings, Ontario Petroleum Institute, 28th annual conference, 28, Technical Paper 16.* London, Ontario.

Faure, & Gunter. (1991). *Principles and applications of inorganic geochemistry: A comprehensive textbook for geology students.* New York, NY: Macmillan Publication Co.

Faure, G. (1986). *Principles of Isotope Geology.* New York, NY: Wiley.

Frape, S. K., Fritz, P., & McNutt, R. H. (1984). The role of water-rock interaction in the chemical evolution of groundwaters from the Canadian Shiels. *Geochimica et Cosmochimica Acta, 48*, 1617-1627.

Ganguly, A. (2012). *Fundamentals of Inorganic Chemistry* (2nd ed.). New Delhi, India: Pearson.

Google Maps. (2014). *Google Maps*. Retrieved Jan 15, 2014, from Google Maps: http://maps.google.ca

Gosselin, D. C., Harvey, F. H., Frost, C., Stotler, R., & Macfarlane, P. A. (2004). Strontium isotope geochemistry of groundwater in the central part of the Dakota (Great Plains) aquifer, USA. *Applied Geochemistry, 19*, 349-377.

Heagle, D., & Pinder, L. (2009). *Opportunistic Groundwater Sampling in DGR-3 and DGR-4, Technical Report TR-08-18.* DGR Site Characterization Document, Intera Engineering, Toronto.

Hodell, D. A., Mead, G. A., & Mueller, P. A. (1990). Variation in the strontium isotopic composition of seawater (8 Ma to present) : Implications for chemical weathering rates and dissolved fluxes to the oceans. *Chemical Geology : Isotope Geoscience section, 80*, 291-307.

Holden, N. E. (2004). Section 11 : Table of the Isotopes. In W. M. (dir.), *CRC Handbook of Chemistry and Physics* (85th ed.). Boca Raton, Florida: CRC Press.

Holland, H. D. (1984). *The Chemical Evolution of the Atmospheres and Ocean.* Princeton, NJ: Princeton University.

Isotope Geochemistry and Geochronology Research Centre. (2013). *Rb/Sr/REE Extraction Procedure With Dowex 50-X8 Cation Resin.* Carleton University.

Jackson, R., & Heagle, D. (2010). *Opportunistic Groundwater Sampling in DGR-1 & DGR-2, Technical Report TR-07-11*. DGR Site Characterization Document, Intera Engineering, Toronto.

Jackson, R., & Murphy, S. (2011). Mineralogical and Lithogeochemical Analyses of DGR-5 and DGR-6 Core, Technical Report TR-09-06. 158.

Jacobson, A. D., Blum, J. D., Page Chamberlain, C., Poage, M. A., & Sloan, V. F. (2002). Ca/Sr and Sr isotope systematics of a Himalayan glacial chronosequence : Carbonate versus silicate weathering rates as a function of landscape surface age. *Geochimica et Cosmochimica Acta, 66*(1), 13-27.

Kobluk, D. R., & Brookfield, M. E. (1982). Excursion 12A : Lower Paleozoic carbonate rocks and paleoenvironments in southern Ontario. *Field Excursion Guidebook*.

Lerouge, C., Gaucher, E. C., Tournassat, C., Negrel, P., Crouzet, C., Guerrot, C., . . . Buschaert, S. (2010). Strontium distribution and origins in a natural clayey formation (Callovian-Oxfordian, Paris Basin, France): A new sequential extraction procedure. *Geochimica et Cosmochimica Acta, 74*, 2926-2942.

Li, D., Shields-Zhou, G. A., Ling, H.-F., & Thirlwall, M. (2011). Dissolution methods for strontium isotope stratigraphy: Guidelines for the use of bulk carbonate and phosphorite rocks. *Chemical Geology, 290*, 133-144.

Lide, D. R. (2005). Section 14 : Geophysics, Astronomy, and Acoustics; Abundance of Elements in the Earth's Crust and in the Sea. In W. M. Haynes, *CRC Handbook of Chemistry and Physics* (85th ed.). Boca Raton, Florida: CRC Press.

Macauley, G., Fowler, M. G., Goodarzi, F., Snowdon, L. R., & Stasiuk, L. D. (1990). Ordovician oil shale-source rock sediments in the central and eastern Canada mainland and eastern arctic areas, and their significance for frontier exploration. *Geological Survey of Canada, Paper 90-14*.

McNutt, R. H., Frape, S. K., & Fritz, P. (1984). Strontium isotopic composition of some brines from the Precambrian Shield of Canada. *Isotope Geoscience, 2*, 205-215.

National Aeronautics and Space Administration. (2012). *WMAP - Age of the Universe*. Retrieved Februrary 19, 2014, from National Aeronautics and Space Administration: http://map.gsfc.nasa.gov/universe/uni_age.html

Nelson, S. A. (2013). *Radiometric Dating*. Retrieved 02 19, 2014, from Tulane University, Earth & Environmental Sciences 2110, Mineralogy: http://www.tulane.edu/~sanelson/eens211/radiometric_dating.htm

Papanastassiou, D. A., Wasserburg, G. J., & Burnett, D. S. (1969). Initial strontium isotopic abundances and the resolution of small time differences in the formation of planetary objects. *Earth Planetary Science Letters, 5*, 361-76.

Patchett, P. J., & Samson, S. D. (2003). Ages and growth of the continental crust from radiogenic isotopes. (H. D. Holland, & K. K. Turekian, Eds.) *Treatise on Geochemistry, 3*, 321-348.

Raven, K., McCreath, D., Jackson, R., Clark, I., Heagle, D., Sterling, S., & Melaney, M. (2011). *OPG's Deep Geologic Repository for Low & Intermediate Level Waste : Descriptive Geosphere Site Model, NWMO DGR-TR-2011-24.* Intera Engineering Ltd. & Nuclear Waste Management Organization, Toronto.

Reardon, E. J., & Armstrong, D. K. (1987). Celestite solubility in water, seawater and NaCl solution. *Geochimica et Cosmochimica Acta, 51*(1), 63-72.

Rotenberg, E., Davis, D. W., Amelin, Y., Ghosh, S., & Bergquist, B. A. (2012). Determination of the decay-constant of 87Rb by laboratory accumulation of 87Sr. *Geochimica et Cosmochimica Acta, 85*(15), 41-57.

Shannon, R. D. (1976). Revised effective ionic radii and systematic studies of interatomic distances in halides and chalcogenides. *Acta Crystallographica Section A, A32*, 751-67.

Sharp, M., Creaser, R. A., & Skidmore, M. (2002). Strontium isotope composition of runoff from a glaciated carbonate terrain. *Geochimica et Cosmochimica Acta, 66*(4), 595-614.

Spencer, E. A. (2013). Personal communication, University of Ottawa.

Sposito, G. (1989). *The Chemistry of Soils.* New York, NY: Oxford Univ. Press.

Tessier, A., Campbell, P., & Bisson, M. (1979). Sequential Extraction Procedure for the Speciation of Particulate Trace Metals. *Analytical Chemistry, 51*(7), 844-851.

Veizer, J. (1989). Strontium isotopes in seawater through time. *Annual Review of Earth and Planetary Science, 17*, 141-167.

Veizer, J. (1992). Depositional and diagenetic History of Limestones : Stable and Radiogenic Isotopes. (N. Clauer, & S. Chaudhuri, Eds.) *Lecture Notes in Earth Sciecnces, 43*, 13-48.

Wilson, B. M. (1989). *Igneous Petrogenesis : A Global Tectonic Approach* (1st ed.). Netherlands: Harper Collins Academic.

APPENDIX A:

SR EXTRACTION PROCEDURE WITH CATION RESIN

PROCEDURE

1. Remove parafilm and caps from orange columns, let columns drain.
2. Sample should have been dissolved overnight in 1.5 ml 2.5N HCl, preferably on a 90°C hotplate. Label centrifuge tubes and centrifuge samples for at least 4 minutes.
3. Add samples to columns with 0.5ml pipette, being careful to get drops to fall to the top of the resin bed without touching the column walls. Do not let the pipette tip seal against the top of the column, or you will create a vacuum in the column when you let up on the pipette plunger.
4. Wash down the sides of the column with ~ 1 ml 2.5N HCl by twirling the column with one hand and squirting acid in the top for a couple of seconds with the other.
5. Add 16ml 2.5ml HCl, let drain through.
6. Place clean, labelled snap-cap beaker under column, and discard acid in waste bucket. Leave snap-cap lids on the carousel.
8. Add 6ml 2.5N HCl, collect in snap-cap beaker (the Sr fraction). When complete, put on hot-plate to dry. Replace waste bucket under column.

CLEANING

Add 3 column volumes of 6N HCl; resin shrinks. Add one column volume of ~ 2N HCl, resin epands. Add 8ml 2.5N HCl (half-way up the yellow buckets), resin equilibrates. Cut parafilm to seal the base of the columns, add ~ 2mls 2.5N HCl to the columns to keep them wet, and put the caps back on the top.

(Isotope Geochemistry and Geochronology Research Centre, 2013)

APPENDIX B:

CALCULATED $^{87}SR/^{86}SR$ INGROWTH IN ROCKS

Table B.1: Calculated ingrowth of ^{87}Sr in water leachates

Sample ID	Depth (mBGS DGR-1/2)	[Rb] (mmol/kg)	[Sr] (mmol/kg)	^{87}Rb (t=0) (mmol/kg)	^{87}Sr (t=0) (mmol/kg)	^{86}Sr (t=0) (9.86%) (mmol/kg)	$^{87}Sr/^{86}Sr$ (t=0)	^{87}Sr ingr. (mmol/kg)	^{87}Sr (t=450 my) (mmol/kg)	$^{87}Sr/^{86}Sr$ (t=450 my)	$^{87}Sr/^{86}Sr$ meas.	$^{87}Rb/^{86}Sr$
5-497.50	458.01	0.039	0.0496	0.01094	0.00346	0.0049	0.7080	0.000069	0.0035	0.7220	0.7230	2.2381
5-525.57	484.59	0.017	0.0589	0.00486	0.00411	0.0058	0.7080	0.000031	0.0041	0.7132	0.7137	0.8364
5-564.96	522.20	0.008	0.0521	0.00213	0.00363	0.0051	0.7080	0.000013	0.0036	0.7105	0.7119	0.4150
5-598.37	554.92	0.015	0.0379	0.00417	0.00265	0.0037	0.7080	0.000026	0.0027	0.7149	0.7234	1.1155
5-625.23	581.28	0.012	0.0625	0.00324	0.00436	0.0062	0.7080	0.000020	0.0044	0.7112	0.7122	0.5252
6-662.17	589.41	0.008	0.0190	0.00221	0.00132	0.0019	0.7080	0.000014	0.0013	0.7154	0.7115	1.1801
5-715.60	666.57	0.004	0.0235	0.00109	0.00164	0.0023	0.7080	0.000007	0.0017	0.7109	0.7097	0.4677
5-719.91	676.15	0.003	0.0299	0.00087	0.00208	0.0029	0.7080	0.000005	0.0021	0.7098	0.7095	0.2941
5-731.02	682.45	0.005	0.0278	0.00129	0.00194	0.0027	0.7080	0.000008	0.0020	0.7109	0.7105	0.4713
5-734.06	685.58	0.003	0.0325	0.00090	0.00227	0.0032	0.7080	0.000006	0.0023	0.7097	0.7094	0.2822

Table B.2: Calculated ingrowth of ^{87}Sr in acetic acid leachates

Sample ID	Depth (mBGS DGR-1/2)	[Rb] (mmol/kg)	[Sr] (mmol/kg)	^{87}Rb (t=0) (mmol/kg)	^{87}Sr (t=0) (mmol/kg)	^{86}Sr (t=0) (9.86%) (mmol/kg)	$^{87}Sr/^{86}Sr$ (t=0)	^{87}Sr ingr. (mmol/kg)	^{87}Sr (t=450 my) (mmol/kg)	$^{87}Sr/^{86}Sr$ (t=450 my)	$^{87}Sr/^{86}Sr$ meas.	$^{87}Rb/^{86}Sr$
5-497.50	458.01	0.0124	1.1363	0.00345	0.07932	0.1120	0.7080	0.000022	0.0793	0.7082	0.7092	0.0308
5-525.57	484.59	0.0104	1.5264	0.00290	0.10655	0.1505	0.7080	0.000018	0.1066	0.7081	0.7089	0.0193
5-564.96	522.20	0.0102	1.0449	0.00284	0.07294	0.1030	0.7080	0.000018	0.0730	0.7082	0.7090	0.0276
5-598.37	554.92	0.0103	0.7487	0.00287	0.05226	0.0738	0.7080	0.000018	0.0523	0.7082	0.7103	0.0389
5-625.23	581.28	0.0093	0.3758	0.00259	0.02623	0.0371	0.7080	0.000016	0.0263	0.7084	0.7105	0.0698
6-662.17	589.41	0.0061	2.4277	0.00169	0.16947	0.2394	0.7080	0.000011	0.1695	0.7080	0.7085	0.0071
5-715.60	666.57	0.0034	2.2522	0.00095	0.15722	0.2221	0.7080	0.000006	0.1572	0.7080	0.7082	0.0043
5-719.91	676.15	0.0028	2.0612	0.00077	0.14389	0.2032	0.7080	0.000005	0.1439	0.7080	0.7082	0.0038
5-731.02	682.45	0.0055	2.9726	0.00152	0.20751	0.2931	0.7080	0.000010	0.2075	0.7080	0.7081	0.0052
5-734.06	685.58	0.0030	2.5407	0.00084	0.17737	0.2505	0.7080	0.000005	0.1774	0.7080	0.7081	0.0034

Table B.3: Calculated ingrowth of ^{87}Sr in HCl lechates

Sample ID	Depth (mBGS DGR-1/2)	[Rb] (mmol/kg)	[Sr] (mmol/kg)	^{87}Rb (t=0) (mmol/kg)	^{87}Sr (t=0) (mmol/kg)	^{86}Sr (t=0) (9.86%) (mmol/kg)	$^{87}Sr/^{86}Sr$ (t=0)	^{87}Sr ingr. (mmol/kg)	^{87}Sr (t=450 my) (mmol/kg)	$^{87}Sr/^{86}Sr$ (t=450 my)	$^{87}Sr/^{86}Sr$ meas.	$^{87}Rb/^{86}Sr$
5-497.50	458.01	0.1097	0.1102	0.03052	0.00769	0.0109	0.7080	0.000192	0.0079	0.7256	0.7263	2.8085
5-525.57	484.59	0.0809	0.3355	0.02252	0.02342	0.0331	0.7080	0.000142	0.0236	0.7122	0.7115	0.6807
5-564.96	522.20	0.0375	0.3292	0.01043	0.02298	0.0325	0.7080	0.000066	0.0230	0.7099	0.7098	0.3214
5-598.37	554.92	0.0646	0.1715	0.01798	0.01197	0.0169	0.7080	0.000113	0.0121	0.7146	0.7141	1.0632
5-625.23	581.28	0.0608	0.1584	0.01691	0.01106	0.0156	0.7080	0.000107	0.0112	0.7147	0.7136	1.0827
6-662.17	589.41	0.0290	0.7415	0.00808	0.05176	0.0731	0.7080	0.000051	0.0518	0.7086	0.7092	0.1104
5-715.60	666.57	0.0163	3.2223	0.00452	0.22492	0.3177	0.7080	0.000029	0.2249	0.7080	0.7080	0.0142
5-719.91	676.15	0.0132	2.8860	0.00367	0.20144	0.2846	0.7080	0.000023	0.2015	0.7080	0.7080	0.0129
5-731.02	682.45	0.0193	2.2508	0.00538	0.15711	0.2219	0.7080	0.000034	0.1571	0.7081	0.7081	0.0242
5-734.06	685.58	0.0125	2.5010	0.00349	0.17457	0.2466	0.7080	0.000022	0.1746	0.7080	0.7080	0.0142

Table B.4: Calculated ingrowth of ^{87}Sr in HF/HNO_3 dissolutions

Sample ID	Depth (mBGS DGR-1/2)	[Rb] (mmol/kg)	[Sr] (mmol/kg)	^{87}Rb (t=0) (mmol/kg)	^{87}Sr (t=0) (mmol/kg)	^{86}Sr (t=0) (9.86%) (mmol/kg)	$^{87}Sr/^{86}Sr$ (t=0)	^{87}Sr ingr. (mmol/kg)	^{87}Sr (t=415 my) (mmol/kg)	$^{87}Sr/^{86}Sr$ (t=415 my)	$^{87}Sr/^{86}Sr$ meas.	$^{87}Rb/^{86}Sr$
5-497.50	458.01	1.2138	0.3001	0.33781	0.02095	0.0296	0.7080	0.001964	0.0229	0.7743	0.7924	11.4170
5-525.57	484.59	1.5604	0.2593	0.43426	0.01810	0.0256	0.7080	0.002525	0.0206	0.8067	0.7936	16.9850
5-564.96	522.20	1.1628	0.2411	0.32360	0.01683	0.0238	0.7080	0.001881	0.0187	0.7870	0.7823	13.6103
5-598.37	554.92	0.3550	0.0851	0.09880	0.00594	0.0084	0.7080	0.000574	0.0065	0.7763	0.7888	11.7685
5-625.23	581.28	0.4929	0.0927	0.13717	0.00647	0.0091	0.7080	0.000797	0.0073	0.7952	0.7807	15.0092
6-662.17	589.41	0.9397	0.2816	0.26151	0.01966	0.0278	0.7080	0.001520	0.0212	0.7627	0.7623	9.4174
5-715.60	666.57	0.3711	0.2618	0.10329	0.01827	0.0258	0.7080	0.000600	0.0189	0.7312	0.7328	4.0018
5-719.91	676.15	0.2889	0.1956	0.08040	0.01365	0.0193	0.7080	0.000467	0.0141	0.7321	0.7342	4.1690
5-731.02	682.45	0.4664	0.1936	0.12979	0.01352	0.0191	0.7080	0.000755	0.0143	0.7474	0.7541	6.7975
5-734.06	685.58	0.2355	0.1521	0.06555	0.01062	0.0150	0.7080	0.000381	0.0110	0.7333	0.7409	4.3702

APPENDIX C:

$^{87}SR/^{86}SR$ INGROWTH FROM GROUNDWATERS

Table C.1: Calculated original $^{87}Sr/^{86}Sr$ values for porewaters

Sample ID	[Rb] (mmol/kg)	[Sr] (mmol/kg)	^{87}Rb (t=x) (mmol/kg)	^{87}Sr (t=x) (mmol/kg)	^{86}Sr (9.86%) (mmol/kg)	$^{87}Sr/^{86}Sr$ meas.	^{87}Sr ingrown (t=415 my) (mmol/kg)	^{87}Rb (t=0) (mmol/kg)	^{87}Sr (t=0) (mmol/kg)	$^{87}Sr/^{86}Sr$ (t=0)
DGR5-497.50	0.1973	12.5879	0.0549	0.8808	1.2412	0.7097	0.000319	0.0552	0.8805	0.7094
DGR 5-514.22	0.2204	11.8418	0.0613	0.8286	1.1676	0.7096	0.000357	0.0617	0.8282	0.7093
DGR 5-525.57	0.2259	13.8559	0.0629	0.9696	1.3662	0.7097	0.000365	0.0632	0.9692	0.7094
DGR 5-557.65	0.1988	11.7838	0.0553	0.8246	1.1619	0.7097	0.000322	0.0556	0.8243	0.7094
DGR 5-564.96	0.2399	17.4436	0.0668	1.2209	1.7199	0.7098	0.000388	0.0672	1.2205	0.7096
DGR 5-598.37	0.2511	11.4331	0.0699	0.8003	1.1273	0.7099	0.000406	0.0703	0.7999	0.7095
DGR 5-625.23	0.2025	12.7742	0.0563	0.8941	1.2595	0.7099	0.000328	0.0567	0.8938	0.7096
DGR 6-654.12	0.2214	17.6451	0.0616	1.2351	1.7398	0.7099	0.000358	0.0620	1.2348	0.7097
DGR 6-661.83	0.1974	16.8220	0.0549	1.1775	1.6587	0.7099	0.000319	0.0552	1.1772	0.7097
DGR 6-662.17	0.2011	19.4805	0.0560	1.3635	1.9208	0.7099	0.000325	0.0563	1.3632	0.7097
DGR 6-662.82	0.1914	16.0861	0.0533	1.1260	1.5861	0.7099	0.000310	0.0536	1.1257	0.7097
DGR 5-649.57	0.1634	14.2253	0.0455	0.9958	1.4026	0.7099	0.000264	0.0457	0.9955	0.7097
DGR 6-683.25	0.1802	14.6662	0.0501	1.0266	1.4461	0.7099	0.000291	0.0504	1.0263	0.7097
DGR 6-697.97	0.2084	19.5379	0.0580	1.3676	1.9264	0.7099	0.000337	0.0583	1.3672	0.7097
DGR 5-671.30	0.1430	13.9241	0.0398	0.9747	1.3729	0.7099	0.000231	0.0400	0.9744	0.7098
DGR 5-683.57	0.1915	19.5373	0.0533	1.3676	1.9264	0.7099	0.000310	0.0536	1.3673	0.7098
DGR 5-697.85	0.1696	17.0141	0.0472	1.1910	1.6776	0.7099	0.000274	0.0475	1.1907	0.7098
DGR 5-715.60	0.0591	19.4800	0.0164	1.3635	1.9207	0.7099	0.000096	0.0165	1.3634	0.7098
DGR 5-724.60	0.0543	20.0800	0.0151	1.4056	1.9799	0.7100	0.000088	0.0152	1.4056	0.7099
DGR 5-731.02	0.0550	11.1500	0.0153	0.7804	1.0994	0.7099	0.000089	0.0154	0.7804	0.7098
DGR 5-734.06	0.1035	17.6100	0.0288	1.2328	1.7363	0.7100	0.000168	0.0290	1.2326	0.7099

Table C.2: Ingrowth from porewaters, starting with the original groundwater mixing line

Sample ID	[Rb] (mmol/kg)	[Sr] (mmol/kg)	^{87}Rb (t=0) (mmol/kg)	^{87}Sr (t=0) (mmol/kg)	^{86}Sr (9.86%) (mmol/kg)	^{87}Sr/^{86}Sr (t=0)	^{87}Sr ingrown (t=415 my) (mmol/kg)	^{87}Rb (t=0) (mmol/kg)	^{87}Sr (t=415 my) (mmol/kg)	^{87}Sr/^{86}Sr (t=415 my)
5-497.50	0.1973	12.5879	0.0549	0.8803	1.2412	0.7093	0.000319	0.0552	0.8806	0.7095
5-514.22	0.2204	11.8418	0.0613	0.8282	1.1676	0.7093	0.000357	0.0617	0.8286	0.7096
5-525.57	0.2259	13.8559	0.0629	0.9691	1.3662	0.7093	0.000365	0.0632	0.9695	0.7096
5-557.65	0.1988	11.7838	0.0553	0.8243	1.1619	0.7094	0.000322	0.0556	0.8246	0.7097
5-564.96	0.2399	17.4436	0.0668	1.2202	1.7199	0.7095	0.000388	0.0672	1.2206	0.7097
5-598.37	0.2511	11.4331	0.0699	0.7999	1.1273	0.7095	0.000406	0.0703	0.8003	0.7099
5-625.23	0.2025	12.7742	0.0563	0.8938	1.2595	0.7096	0.000328	0.0567	0.8941	0.7099
6-654.12	0.2214	17.6451	0.0616	1.2346	1.7398	0.7096	0.000358	0.0620	1.2350	0.7098
6-661.83	0.1974	16.8220	0.0549	1.1770	1.6587	0.7096	0.000319	0.0552	1.1774	0.7098
6-662.17	0.2011	19.4805	0.0560	1.3631	1.9208	0.7096	0.000325	0.0563	1.3634	0.7098
6-662.82	0.1914	16.0861	0.0533	1.1256	1.5861	0.7096	0.000310	0.0536	1.1259	0.7098
5-649.57	0.1634	14.2253	0.0455	0.9954	1.4026	0.7097	0.000264	0.0457	0.9957	0.7099
6-683.25	0.1802	14.6662	0.0501	1.0263	1.4461	0.7097	0.000291	0.0504	1.0266	0.7099
6-697.97	0.2084	19.5379	0.0580	1.3672	1.9264	0.7097	0.000337	0.0583	1.3676	0.7099
5-671.30	0.1430	13.9241	0.0398	0.9744	1.3729	0.7097	0.000231	0.0400	0.9746	0.7099
5-683.57	0.1915	19.5373	0.0533	1.3673	1.9264	0.7098	0.000310	0.0536	1.3676	0.7099
5-697.85	0.1696	17.0141	0.0472	1.1908	1.6776	0.7098	0.000274	0.0475	1.1910	0.7100
5-715.60	0.0591	19.4800	0.0164	1.3634	1.9207	0.7099	0.000096	0.0165	1.3635	0.7099
5-724.60	0.0543	20.0800	0.0151	1.4055	1.9799	0.7099	0.000088	0.0152	1.4056	0.7099
5-731.02	0.0550	11.1500	0.0153	0.7805	1.0994	0.7099	0.000089	0.0154	0.7805	0.7100
5-734.06	0.1035	17.6100	0.0288	1.2327	1.7363	0.7099	0.000168	0.0290	1.2328	0.7100

APPENDIX D:

$^{87}SR/^{86}SR$ INGROWTH FROM SEAWATER

Table D.1: Calculated ingrowth of ^{87}Sr in porewaters, starting with seawater ratio

Sample ID	Seawater $^{87}Sr/^{86}Sr$	[Sr] in porewaters (mmol/kg)	[^{86}Sr] in porewater (9.86% natural abundance) (mmol/kg)	[^{87}Sr] in porewater (mmol/kg)	[^{87}Rb] in porewater (mmol/kg)	[^{87}Sr] ingrowth from ^{87}Rb-decay in porewater (t= 450 m.y.)	[^{87}Sr] final in porewaters, after ingrowth (mmol/kg)	Final $^{97}Sr/^{86}Sr$ in porewaters
5-497.50	0.7080	12.588	1.2412	0.8786	0.0549	0.000346	0.8790	0.7082
5-514.22	0.7080	11.842	1.1676	0.8266	0.0613	0.000387	0.8269	0.7082
5-525.57	0.7080	13.856	1.3662	0.9671	0.0629	0.000396	0.9675	0.7082
5-557.65	0.7080	11.784	1.1619	0.8225	0.0553	0.000349	0.8229	0.7082
5-564.96	0.7080	17.444	1.7199	1.2176	0.0668	0.000421	1.2180	0.7082
5-598.37	0.7080	11.433	1.1273	0.7980	0.0699	0.000441	0.7985	0.7083
5-625.23	0.7080	12.774	1.2595	0.8916	0.0563	0.000355	0.8920	0.7082
6-654.12	0.7080	17.645	1.7398	1.2316	0.0616	0.000388	1.2320	0.7081
6-661.83	0.7080	16.822	1.6587	1.1742	0.0549	0.000346	1.1745	0.7081
6-662.17	0.7080	19.481	1.9208	1.3597	0.0560	0.000353	1.3601	0.7081
6-662.82	0.7080	16.086	1.5861	1.1228	0.0533	0.000336	1.1232	0.7081
5-649.57	0.7080	14.225	1.4026	0.9929	0.0455	0.000287	0.9932	0.7081
6-683.25	0.7080	14.666	1.4461	1.0237	0.0501	0.000316	1.0240	0.7081
6-697.97	0.7080	19.538	1.9264	1.3637	0.0580	0.000366	1.3641	0.7081
5-671.30	0.7080	13.924	1.3729	0.9719	0.0398	0.000251	0.9722	0.7081
5-683.57	0.7080	19.537	1.9264	1.3637	0.0533	0.000336	1.3640	0.7081
5-697.85	0.7080	17.014	1.6776	1.1876	0.0472	0.000298	1.1879	0.7081
5-715.60	0.7080	19.480	1.9207	1.3597	0.0164	0.000104	1.3598	0.7080
5-724.60	0.7080	20.080	1.9799	1.4016	0.0151	0.000095	1.4017	0.7080
5-731.02	0.7080	11.150	1.0994	0.7783	0.0153	0.000097	0.7784	0.7080
5-734.06	0.7080	17.610	1.7363	1.2292	0.0288	0.000182	1.2294	0.7080

Table D.2: Calculated ingrowth of ^{87}Sr in porewaters from H_2O leachate, starting with seawater ratio

Sample ID	Seawater $^{87}Sr/^{86}Sr$	[Sr] in water leachate (mmol/kg)	[^{86}Sr] in water leachate (9.86%) (mmol/kg)	[^{87}Sr] in water leachate (mmol/kg)	[^{87}Rb] in water leachate (mmol/kg)	[^{87}Sr] ingrowth from ^{87}Rb-decay in water leachate (t= 450 m.y.)	[^{87}Sr] final in porewaters, after ingrowth[1] (mmol/kg)	Final $^{97}Sr/^{86}Sr$ in porewaters[2]
DGR5-497.50	0.7080	0.0496	0.0049	0.00346	0.01094	0.000070	0.8792	0.7083
DGR5-525.57	0.7080	0.0589	0.0058	0.00411	0.00486	0.000031	0.9677	0.7083
DGR5-564.96	0.7080	0.0521	0.0051	0.00363	0.00213	0.000014	1.2182	0.7082
DGR5-598.37	0.7080	0.0379	0.0037	0.00265	0.00417	0.000027	0.7986	0.7084
DGR5-625.23	0.7080	0.0625	0.0062	0.00436	0.00324	0.000021	0.8921	0.7083
DGR6-662.17	0.7080	0.0190	0.0019	0.00132	0.00221	0.000014	1.3603	0.7082
DGR5-715.60	0.7080	0.0235	0.0023	0.00164	0.00109	0.000007	1.3600	0.7081
DGR5-724.60	0.7080	0.0299	0.0029	0.00208	0.00087	0.000006	1.4019	0.7080
DGR5-731.02	0.7080	0.0278	0.0027	0.00194	0.00129	0.000008	0.7785	0.7081
DGR5-734.06	0.7080	0.0325	0.0032	0.00227	0.00090	0.000006	1.2295	0.7081

[1]Combined ingrowth from the porewater and the water leachate
[2]Considering decay from Rb in porewater and in water leachate

Table D.3: Calculated ingrowth of ^{87}Sr in porewaters from AcOH leachate, starting with seawater ratio

Sample ID	Seawater $^{87}Sr/^{86}Sr$	[Sr] in AcOH leachate (mmol/kg)	[^{86}Sr] in AcOH leachate (9.86%) (mmol/kg)	[^{87}Sr] in AcOH leachate (mmol/kg)	[^{87}Rb] in AcOH leachate (mmol/kg)	[^{87}Sr] ingrowth from ^{87}Rb-decay in AcOH leachate (t= 450 m.y.)	[^{87}Sr] final in porewaters, after ingrowth[1] (mmol/kg)	Final $^{97}Sr/^{86}Sr$ in porewaters[2]
DGR5-497.50	0.7080	1.1363	0.1120	0.07931	0.00345	0.000022	0.8791	0.7083
DGR5-525.57	0.7080	1.5264	0.1505	0.10654	0.00290	0.000019	0.9677	0.7083
DGR5-564.96	0.7080	1.0449	0.1030	0.07293	0.00284	0.000018	1.2182	0.7083
DGR5-598.37	0.7080	0.7487	0.0738	0.05226	0.00287	0.000018	0.7986	0.7084
DGR5-625.23	0.7080	0.3758	0.0371	0.02623	0.00259	0.000017	0.8921	0.7083
DGR6-662.17	0.7080	2.4277	0.2394	0.16945	0.00169	0.000011	1.3603	0.7082
DGR5-715.60	0.7080	2.2522	0.2221	0.15720	0.00095	0.000006	1.3600	0.7081
DGR5-724.60	0.7080	2.0612	0.2032	0.14387	0.00077	0.000005	1.4019	0.7081
DGR5-731.02	0.7080	2.9726	0.2931	0.20749	0.00152	0.000010	0.7785	0.7081
DGR5-734.06	0.7080	2.5407	0.2505	0.17734	0.00084	0.000005	1.2295	0.7081

[1]Combined ingrowth from the porewater and the AcOH leachate
[2]Considering decay from Rb in porewater and in AcOH leachate

Table D.4: Calculated ingrowth of ^{87}Sr in porewaters from HCl leachate, starting with seawater ratio

Sample ID	Seawater $^{87}Sr/^{86}Sr$	[Sr] in HCl leachate (mmol/kg)	[^{86}Sr] in HCl leachate (9.86%) (mmol/kg)	[^{87}Sr] in HCl leachate (mmol/kg)	[^{87}Rb] in HCl leachate (mmol/kg)	[^{87}Sr] ingrowth from ^{87}Rb-decay in HCl leachate (t= 450 m.y.)	[^{87}Sr] final in porewaters, after ingrowth[1] (mmol/kg)	Final $^{97}Sr/^{86}Sr$ in porewaters[2]
DGR5-497.50	0.7080	0.1102	0.0109	0.00769	0.03052	0.000196	0.8793	0.7084
DGR5-525.57	0.7080	0.3355	0.0331	0.02342	0.02252	0.000144	0.9678	0.7084
DGR5-564.96	0.7080	0.3292	0.0325	0.02298	0.01043	0.000067	1.2182	0.7083
DGR5-598.37	0.7080	0.1715	0.0169	0.01197	0.01798	0.000115	0.7987	0.7085
DGR5-625.23	0.7080	0.1584	0.0156	0.01106	0.01691	0.000108	0.8922	0.7084
DGR6-662.17	0.7080	0.7415	0.0731	0.05176	0.00808	0.000052	1.3603	0.7082
DGR5-715.60	0.7080	3.2223	0.3177	0.22492	0.00452	0.000029	1.3600	0.7081
DGR5-724.60	0.7080	2.8860	0.2846	0.20144	0.00367	0.000024	1.4019	0.7081
DGR5-731.02	0.7080	2.2508	0.2219	0.15711	0.00538	0.000034	0.7785	0.7081
DGR5-734.06	0.7080	2.5010	0.2466	0.17457	0.00349	0.000022	1.2295	0.7081

[1]Combined ingrowth from the porewater and the HCl leachate
[2]Considering decay from Rb in porewater and in HCl leachate

Table D.5: Calculated ingrowth of ^{87}Sr in porewaters from HF/HNO_3 dissolution, starting with seawater ratio

Sample ID	Seawater $^{87}Sr/^{86}Sr$	[Sr] in HF/HNO_3 dissolution (mmol/kg)	[^{86}Sr] in HF/HNO_3 dissolution (9.86%) (mmol/kg)	[^{87}Sr] in HF/HNO_3 dissolution (mmol/kg)	[^{87}Rb] in HF/HNO_3 dissolution (mmol/kg)	[^{87}Sr] ingrowth from ^{87}Rb-decay in HF/HNO_3 (t= 450 m.y.)	[^{87}Sr] final in porewaters, after ingrowth[1] (mmol/kg)	Final $^{97}Sr/^{86}Sr$ in porewaters[2]
DGR5-497.50	0.7080	0.3001	0.0296	0.02095	0.33781	0.002165	0.8813	0.7100
DGR5-525.57	0.7080	0.2593	0.0256	0.01810	0.43426	0.002784	0.9704	0.7103
DGR5-564.96	0.7080	0.2411	0.0238	0.01683	0.32360	0.002074	1.2202	0.7095
DGR5-598.37	0.7080	0.0851	0.0084	0.00594	0.09880	0.000633	0.7992	0.7090
DGR5-625.23	0.7080	0.0927	0.0091	0.00647	0.13717	0.000879	0.8930	0.7090
DGR6-662.17	0.7080	0.2816	0.0278	0.01966	0.26151	0.001676	1.3619	0.7091
DGR5-715.60	0.7080	0.2618	0.0258	0.01827	0.10329	0.000662	1.3606	0.7084
DGR5-724.60	0.7080	0.1956	0.0193	0.01365	0.08040	0.000515	1.4024	0.7083
DGR5-731.02	0.7080	0.1936	0.0191	0.01352	0.12979	0.000832	0.7793	0.7088
DGR5-734.06	0.7080	0.1521	0.0150	0.01062	0.06555	0.000420	1.2299	0.7083

[1]Combined ingrowth from the porewater and the HF/HNO_3 dissolution
[2]Considering decay from Rb in porewater and in HF/HNO_3 dissolution

Table D.6: Calculated ingrowth of ^{87}Sr in porewaters from the whole rock, starting with seawater ratio

Sample ID	Seawater $^{87}Sr/^{86}Sr$	[Sr] in whole rock (mmol/kg)	[^{86}Sr] in whole rock (9.86%) (mmol/kg)	[^{87}Sr] in whole rock (mmol/kg)	[^{87}Rb] in whole rock (mmol/kg)	[^{87}Sr] ingrowth from ^{87}Rb-decay in whole rock (t= 450 m.y.)	[^{87}Sr] final in porewaters, after ingrowth[1] (mmol/kg)	Final $^{97}Sr/^{86}Sr$ in porewaters[2]
DGR5-497.50	0.7080	1.59612	0.15738	0.11141	0.38272	0.002453	0.8816	0.7103
DGR5-525.57	0.7080	2.18011	0.21496	0.15217	0.46454	0.002978	0.9706	0.7105
DGR5-564.96	0.7080	1.66732	0.16440	0.11638	0.33901	0.002173	1.2203	0.7095
DGR5-598.37	0.7080	1.04324	0.10286	0.07282	0.12382	0.000794	0.7994	0.7091
DGR5-625.23	0.7080	0.68943	0.06798	0.04812	0.15990	0.001025	0.8931	0.7091
DGR6-662.17	0.7080	3.46978	0.34212	0.24219	0.27348	0.001753	1.3620	0.7091
DGR5-715.60	0.7080	5.75977	0.56791	0.40203	0.10985	0.000704	1.3607	0.7084
DGR5-724.60	0.7080	5.17268	0.51003	0.36105	0.08571	0.000549	1.4024	0.7083
DGR5-731.02	0.7080	5.44487	0.53686	0.38005	0.13798	0.000885	0.7794	0.7089
DGR5-734.06	0.7080	5.22629	0.51531	0.36479	0.07078	0.000454	1.2300	0.7084

[1]Combined ingrowth from the porewater and whole rock
[2]Considering decay from Rb in porewater and in whole rock